

Climate regime of Asian glaciers revealed by GAMDAM Glacier Inventory

A. Sakai¹, T. Nuimura^{1,*}, K. Fujita¹, S. Takenaka¹, H. Nagai^{1,**}, D. Lamsal¹

[1]{Graduate School of Environmental Studies, Nagoya University, Nagoya, Japan}

[*]{now at: Chiba Institute of Science, Chiba, Japan}

[**]{now at: Earth Observation Research Center, Japan Aerospace Exploration Agency,
Tsukuba, Japan}

Correspondence to: A. Sakai (shakai@nagoya-u.jp)

Abstract

Among meteorological elements, precipitation has a large spatial variability and less observation, particularly in High Mountain Asia, although precipitation in mountains is an important parameter for hydrological circulation. We estimated precipitation contributing to glacier mass at median elevation of glaciers, which is presumed to be at equilibrium-line altitude (ELA) so that mass balance is zero at that elevation, by tuning adjustment parameters of precipitation. We also made comparisons between median elevation of glaciers, including the effect of drifting snow and avalanche, and eliminated those local effects. Then, we could obtain median elevation of glaciers depending only on climate to estimate glacier surface precipitation.

The calculated precipitation contributing to glacier mass can elucidate that glaciers in the arid High Mountain Asia receive less precipitation, while much precipitation makes a greater contribution to glacier mass in the Hindu Kush, the Himalayas, and the Hengduan Shan due to not only direct precipitation amount but also avalanche nourishment. We classified glaciers in High Mountain Asia into summer-accumulation type and winter-accumulation type using the summer accumulation ratio, and confirmed that summer-accumulation type glaciers have a higher sensitivity than winter-accumulation type glaciers.

1 Introduction

Meltwater from glaciers and seasonal snow in the high mountains is a significant water resource in Asia (Immerzeel et al., 2010, 2013; Kaser et al., 2010). However, Asian

1 mountains have a poor network of precipitation measurement (Bookhagen and Burbank,
2 2006), even though precipitation is a crucial parameter for understanding hydrological
3 processes. In addition, meteorological stations in mountain regions are generally located at
4 lower elevations in the valleys, and thus are not representative of basin-scale precipitation
5 because of strong orographic effects. Several gridded datasets compiling precipitation have
6 been produced based on ground rain-gauge data or satellite data on a global scale (Chen et al.,
7 2002; New et al., 2000; Huffman et al., 1997). Almost all datasets, however, do not consider
8 orographic effects (Adam et al., 2006).

9 Yatagai et al. (2009, 2012) provided the Asian Precipitation—Highly Resolved
10 Observational Data Integration Towards Evaluation of Water Resources (APHRODITE)
11 gridded precipitation dataset based on gauge data from 1951 to 2007. They interpolated
12 precipitation in mountain regions by considering orographic effects on precipitation based on
13 the parameter-elevation regressions on independent slopes model (Daly et al., 1994). The
14 gridded datasets, however, have significant biases against point observational data in the
15 Himalayan Mountains (Fujita and Nuimura, 2011).

16 Observed precipitation data at high altitude (Putkonen, 2004) is very rare in the High
17 Mountain Asia. Böhner (2006) has generated high resolution climatic data sets, radiation,
18 temperature and precipitation in Central and high Asia. He reported that there are
19 uncertainties in annual water balance owing to methodical limits in the spatial estimation of
20 precipitation in High Mountain Asia. Recently, Maussion et al. (2014) have generated a new
21 high-resolution atmospheric dataset, High Asia Reanalysis (HAR) using Weather Research
22 and Forecasting (WRF) model from October 2000 to September 2011. The HAR reproduced
23 well previously reported spatial pattern and seasonality of precipitation. They proposed a new
24 classification based on precipitation seasonality. Furthermore, they found glaciers of varying
25 types over very short distances in the Himalayan ranges.

26 Braithwaite and Raper (2002) indicated that calibrated precipitation at equilibrium-line
27 altitude (ELA) (Braithwaite and Zhang, 1999) using the degree-day model was considerably
28 greater than the grid precipitation in New et al. (1999) in New Zealand, the Caucasus, the
29 Alps, southern Norway, northern Scandinavia, Svalbard, and Axel Heiberg Island. Engelhart
30 et al. (2012) calculated spatial distribution of glacier mass balances using gridded temperature
31 and precipitation, and then compared the calculated distribution with observed spatial
32 distribution. They indicated that the gridded precipitation did not represent orographic

1 enhancement of precipitation. Rupper and Roe (2008) estimated ELA by the energy mass
2 balance model, with the NCEP/NCAR reanalysis data at High Mountain Asia, assuming all
3 precipitation as solid. However, the estimated ELA had a large discrepancy with glacier
4 distribution. They noted that the reanalysis temperature was a valuable estimator of summer
5 balance, but the reanalysis precipitation was a poor estimator of winter balance. Rasmussen
6 (2013) also pointed out that correlation between the NCEP/NCAR reanalysis precipitation
7 values and winter balance was low. Braithwaite et al. (2006) estimated accumulation at ELA
8 of 180 glaciers using the degree-day model, in which the modelled annual accumulation
9 represented the observed winter balance well. Immerzeel et al. (2012) estimated detailed
10 distribution of precipitation on the Karakoram glaciers by assuming a neutral glacier mass
11 balance. Overall, precipitation in the gridded data still required calibration to calculate glacier
12 mass balance, because amount and seasonality of precipitation strongly affect the sensitivity
13 of glacier mass balance (Oerlemans and Fortuin, 1992; Braithwaite and Raper, 2002; Fujita,
14 2008a, 2008b).

15 The objective of this study was to estimate precipitation at the ELA over Asian glaciers
16 derived from the Glacier Area Mapping for Discharge in Asian Mountains (GAMDAM)
17 Glacier Inventory (GGI) (Nuimura et al., 2014), and to evaluate the climate regime at the
18 Asian glaciers. We confirmed that median elevation of glaciers can be proxy data for ELA in
19 the Asian glaciers, and established a method for calculating precipitation at median elevation
20 of glaciers by applying a climatic glacier mass balance model with reanalysis dataset, so that
21 mass balance would be zero, by tuning annual precipitation.

22 **2 Study region, data, and method**

23 **2.1 Study region**

24 Our study region covers High Mountain Asia (26.5°–55.5° N, 66.5°–104.5° E), which
25 corresponds to the regions of Central Asia, South Asia West, South Asia East, and Altay and
26 Sayan of North Asia in the Randolph Glacier Inventory (Pfeffer et al., 2014) (Fig. 1). The
27 centre of our target region is the Tibetan Plateau, whose elevation is around 5000 m a.s.l.. The
28 plateau forms an orographic obstacle for westerlies and Indian monsoons. Indian monsoon
29 supply high amounts of precipitation over the Himalaya, but most moisture is orographically
30 forced out at elevations less than 4000 m a.s.l. and the high altitude glacier area are
31 significantly more arid (Harper and Humphrey, 2003). Monsoon moisture influence decreases

1 from east to west along the Himalayas, and Westerlies moisture becomes important in the
2 West Himalayas and the Karakoram. The moisture boundary between monsoon and westerly
3 lies at 78° E near the Sutlej Valley (Bookhagen and Burbank, 2010). Westerlies can reach
4 higher elevation than the summer monsoon, which may be related to the higher tropospheric
5 extent of the westerly airflow (Scherler et al., 2011). Precipitation increases with altitude and
6 maximum precipitation occurs between 5000 and 6000 m a.s.l. (Wake, 1989; Young and
7 Schmok, 1989; Young and Hewitt, 1990; Hewitt, 2011).

8 The Pamir Mountains, located at a transition zone, are influenced by the monsoon and the
9 Westerlies. In the eastern part, the climate is characterised as semiarid and arid mountain
10 climate because the area is surrounded by high mountains (Hindu Kush, Alay, Tien Shan, and
11 Karakoram Mountains) (Zech et al., 2005). The Tien Shan range constitutes the first montane
12 barrier for northern and western air masses travelling from Siberia and the Kazakh steppes to
13 Central Asia. The resulting barrier effects lead to a distinct continentality gradient with
14 decreasing precipitation rates. Sorg et al. (2012) summarized that Western and Northern Tien
15 Shan can be classified as moist regions, and Central Tien Shan and Eastern Tien Shan have a
16 continental arid/semiarid climate. In terms of the seasonality of precipitation, maximum
17 precipitation occurs winter in Western Tien Shan, spring and early summer in Northern and
18 Eastern Tien Shan, and summer in Central Tien Shan.

19 In the Altai range, one of the main factors that determines the climatic regime is
20 interaction between the Siberian High and western cyclonic activity (Surazakov et al., 2007).
21 Aizen et al. (2006a) reported that two-thirds of the accumulation come from oceanic sources
22 (Atlantic or Arctic) and the rest was recycled over Aral-Caspian sources in the Russian Altai
23 Mountains. The Sayan range, located on the northwestern edge of Mongolia, is an
24 arid/semiarid region. Precipitation in Mongolia is supplied by the synoptic-scale disturbances
25 during the summer (June–August) because this region is in the westerly dominant zone. The
26 region contributing to precipitation in Mongolia is western Siberia, located to the northwest of
27 Mongolia. (Sato et al., 2007) Most precipitation in the interior of High Mountain Asia
28 originates from recycled evaporation, and such a proportion of continental recycling cannot be
29 found in the other continents (Yoshimura et al., 2004). These circulation systems characterise
30 the glaciers as summer-accumulation type and winter-accumulation type (Ageta and Higuchi,
31 1984; Fujita and Ageta, 2000).

1 Most glaciers in the Himalayas (Bolch et al., 2012) or on the Tibetan Plateau (Yao et al.,
2 2012) are shrinking, as are glaciers in Tien Shan (Aizen et al., 2006b; Narama et al., 2010;
3 Sorg et al., 2012) and Altai (Surazakov et al., 2007), while glaciers in the Karakoram are in a
4 state of slight mass gain (Gardelle et al., 2013). Furthermore, recent analyses by Kääb et al.
5 (2012), Kääb et al. (2015), Gardner et al. (2013) and Neckel et al. (2014) elucidated that the
6 glacier fluctuations have contrasting behaviours in Asia by repeat ICESat (Ice, Cloud, and
7 land Elevation Satellite) tracks analysis. Fujita and Nuimura (2011) also indicated that the
8 fluctuation of glaciers in High Mountain Asia were spatially heterogeneous, based on
9 calculated ELA with reanalysis datasets.

10 **2.2 Median elevation and ELA derived from GGI**

11 The GGI is a quality controlled glacier outline based on the Landsat level 1 terrain corrected
12 (L1T) scenes, which was delineated manually (Nuimura et al., 2015). Because systematic
13 geometric corrections are performed for the L1T products, the GGI can provide precise
14 hypsometry of glaciers.

15 ELA is defined as the elevation of zero mass balance. Several researchers have proposed
16 different methods for estimating ELA, such as the shape of contour lines and the
17 accumulation area ratio (AAR) method (Torsnes et al., 1993; Benn and Lehmkühl, 2000;
18 Carrivick and Brewer 2004). Braithwaite and Raper (2009) demonstrated the median
19 elevation of 94 glaciers in the World Glacier Inventory (WGI), each with balanced-budget
20 ELA, which is the elevation of zero mass balance for a particular glacier. They showed that
21 median elevations of glaciers (where elevation divides glacier area equally) are available for
22 balanced-budget ELA. Bolch et al. (2012) (Fig. S2) (Himalaya), Paul et al. (2002) (Swiss
23 Alps), Rastner et al. (2012) (Greenland), and Racoviteanu et al. (2008) (Cordillera Blanca in
24 Peru) also show median elevations at each region as an indicator of ELA. In the GLIMS
25 glacier inventory, median elevation is an important basic parameter derived by compiling the
26 glacier polygon data and Digital Elevation Model (Paul et al., 2009).

27 We compared the few observed ELA with median elevation derived from the GGI
28 (Nuimura et al., 2014) using ASTER GDEM (ver. 2) extracted by 30×30 m grid cells
29 (Table S1). Nine glaciers were observed, and the average observed period was 29 years.
30 Figure 2 indicates that decadal ELAs are consistent with the median elevation of each glacier
31 (RMSE = 71; bias = +3), whereas annual ELAs vary widely (RMSE = 114). Nuimura et al.,

1 (2014) also indicated that distribution of the snow line altitude (SLA) of glaciers in China
2 reported by Shi (2008) also corresponded well with median elevation of glaciers derived from
3 the GGI. Those SLAs were estimated from topographic maps by contour inflection (convex in
4 accumulation area and concave in the ablation area) or from aerial photos by average height
5 of firn area margin.

6 **2.3 Median elevation of glaciers as proxy data for ELA**

7 Drifting snow provides a significant contribution to glacier accumulation and affects the
8 present glacier distributions (Jaedicke and Gauer, 2005). Avalanche snow from ice-free slopes
9 is also an important source of glacier accumulation in precipitous terrains (Benn and
10 Lehmkuhl, 2000; Hewitt 2014). Thus, ELA and median elevation of glaciers are affected not
11 only by temperature and precipitation but also by those alternative sources of glacier
12 nourishment.

13 Here, we set three averaged median elevation of glaciers: G-average elevation, L-average
14 elevation, and W-average elevation. We calculate average elevation of glaciers at each
15 0.5×0.5 degree grid by area-weighted averages of median elevation for individual glaciers.
16 The resolution corresponds with that of the precipitation data set (APHRODITE).

17 **2.3.1 G-average elevation**

18 Small glaciers have large variation of median elevation because they have upper or lower
19 distribution when separating from main large glaciers. Furthermore, small glaciers have
20 relatively short response time to climate change (i.e., they would not have recorded climate in
21 the past few decades). Hence, to represent median elevation of large glaciers at each grid cell,
22 we calculate median glacier elevation, area-weighted average at each 0.5-degree grid using
23 the GGI in High Mountain Asia. The minimum glacier area is 0.05 km^2 (Nuimura et al., 2014).
24 Here, we define the simple median glacier elevation as G-average elevation.

25 **2.3.2 L- average elevation**

26 Some median elevations of glaciers averaged at each grid reflect only a few small glaciers.
27 Small glaciers in undulating terrain have been under strong influence of drifting snow and
28 cannot maintain snow or ice mass without drifting snow. Those small glaciers can exist at

1 much lower altitudes than large glaciers. Therefore, we analysed the representativeness of
2 each median elevation of glaciers and the glaciers using the GGI.

3 Median anomaly is the difference between median elevation of each glacier and the
4 average median elevation of the vicinity glaciers. The vicinity glaciers were defined as
5 glaciers located inside the 0.5×0.5 degree grid, with the centre on the location of the glacier,
6 which is defined at the centre of gravity of each glacier. Figure 3a shows that glaciers with a
7 smaller area have large variability of median anomaly. Here, we selected those glaciers with
8 more than 300 glaciers in the vicinity (0.5×0.5 degree grid). In particular, glaciers smaller
9 than 1 km^2 in area have large standard deviations ($\text{STDV} > 230 \text{ m}$) of the median anomaly,
10 and the number of outliers (2σ) is more than 18,000, whereas glaciers larger than 1 km^2 have
11 less than 300 outliers (Figure 3b). This means that smaller glaciers are affected by local
12 terrain.

13 Dahl and Nesje (1992) reported that ELA depression of cirque glaciers is caused by
14 leeward accumulation. Conversely, the windy side of cirque glaciers tend to have higher ELA
15 because of denudation of deposited snow. Furthermore, small glaciers with high median
16 anomalies might be separated glaciers from ablation areas, and those with low median
17 anomalies might be composed of drift snow accumulated by depression. Those with large
18 anomalies of median elevation can be explained by re-distribution of snow because of wind
19 effect or topography.

20 Then, G-average elevations of glaciers are affected by local terrain, in particular, at the
21 grid with only small glaciers. Here, we propose L-average elevation, which is calculated by
22 excluding glaciers smaller than 1 km^2 in area.

23 **2.3.3 W- average elevation**

24 Each median elevation of glaciers is sometimes affected by the geography surrounding the
25 glacier. Scherler et al. (2011) introduced percentage of ice-free areas in the accumulation area
26 and it contributing headwalls as a proxy for the relative importance of avalanche
27 accumulation, and they reported that avalanche-fed glaciers (the percentage of ice-free areas
28 in the accumulation area and it contributing headwalls of a given glacier) have a lower median
29 elevation against snow line elevation in the Himalayas. Steep avalanche walls, at which snow
30 cannot be retained at the surface, were excluded from the GGI (Nuimura et al., 2014). The
31 median elevation of avalanche-fed glaciers would be lowered by the amount of avalanche

1 snow accumulation, which should accumulate at the steep avalanche wall. Then, median
2 elevation of avalanche-fed glaciers calculated from area-altitude distribution, including
3 glaciers as well as steep avalanche walls, would reflect ELA, depending only on temperature
4 and precipitation (not affected by avalanche nourishment). Sensitivity of glacier mass balance
5 to temperature change requires ice or snow mass accumulating on the glacier including not
6 only direct precipitation but also avalanche nourishment. Furthermore, the relation between
7 direct precipitation and ice or snow mass accumulating on the glacier is significant for
8 calculation of glacier mass fluctuation. To estimate direct precipitation on glaciers, we tried to
9 estimate median elevations of glaciers, including steep avalanche walls. Figure S1 shows an
10 example of the estimation of averaged median elevations of glaciers, including steep
11 avalanche walls. We assumed that hypsometry of steep avalanche walls can be estimated by
12 linear interpolation between the area at the altitude of maximum glacier area and maximum
13 ground altitude, at which area is assumed to be zero. Then, averaged median elevation of
14 glaciers, including avalanche walls, became 6125 m (W-average) from 5394 m (L-average).
15 Here, we define the elevation as W-average elevation. When glacier hypsometry higher than
16 median elevation has a strong convex curve, the L-average elevation exceeds the W-average
17 elevation. In this case, W-average elevation is assumed to be equal to L- average elevation.
18 The total number of grids that have different average elevation from L- average elevation is
19 413.

20 **2.4 Meteorological data**

21 **2.4.1 Comparison between observed data and reanalysis dataset**

22 Ablation of glaciers depends on several elements, such as snow, albedo of the glacier
23 surface, air temperature, solar radiation, and longwave radiation. Fujita and Ageta (2000)
24 concluded that the air temperature and solar radiation are the major elements for calculation
25 of glacier ablation. Therefore, daily reanalysis data, air temperature and solar radiation from
26 NCEP/NCAR (Kalnay et al., 1996) and ERA-Interim (Dee et al., 2011) have been compared
27 with the observed data on or adjacent to glaciers in High Mountain Asia (Fig. S2). Analysed
28 site names, locations, and observed periods are summarized in Table S2. Observed
29 meteorological data by **automatic weather station** (AWS), in particular, on the glacier or near
30 the terminus of the glacier are very rare in high Asian mountains. We did not select the
31 observed site, and those daily data are all the data available to us. Air temperature at each

1 AWS (T_o [°C]) were calculated assuming that the free atmosphere air temperatures at each
2 elevation (z_o [m]) (Table S2) is as follows:

$$3 \quad T_z = T_1 + \left(\frac{T_2 - T_1}{z_2 - z_1} \right) \times (z_o - z_1) \quad (1)$$

4 Lapse rate of air temperature is estimated by the temperatures at the two closest
5 geopotential heights (z_1, z_2 [m]) containing the elevation of the AWS (i.e., $z_1 \leq z_o \leq z_2$). T_1 and
6 T_2 (°C) indicate reanalysis air temperatures at each geopotential heights, z_1 and z_2 , respectively.

7 We compared only summer season (JJA) data, because snow cover on the sensors of the
8 instruments tends to impede precise measurement during the winter. Furthermore, calculation
9 of ablation during the melting season has larger effect on glacier mass balance. Both root
10 mean square errors (RMSEs) of solar radiation and temperature between reanalysis and
11 observed data were less for the ERA-Interim. Therefore, we used ERA-Interim for calculation
12 of glacier mass balance as described in the next section.

13

14 **2.4.2 Used reanalysis data**

15 Daily ERA-Interim reanalysis data (Dee et al., 2011), including temperature (level),
16 geopotential height (level), surface wind (surface flux 10 m), surface humidity (surface), and
17 solar radiation (surface flux), from 1952 to 2007, were used to calculate glacier mass balance.
18 The spatial resolution was 0.75×0.75 degrees, and all pressure levels of the temperature and
19 geopotential height data from 300 to 850 hpa (300, 350, 400, 450, 500, 550, 600, 650, 700,
20 750, 775, 800, 825, and 850), which cover all average elevations of each grid, were used.
21 Daily temperatures are given at each average elevation of glaciers, where lapse rate of air
22 temperature is estimated by the temperature at two geopotential heights bounding/containing
23 the average elevation according to Eqn.(1) (z_o should be average elevation for calculation of
24 precipitation). Daily precipitation data, APHRODITE from 1952 to 2007, with spatial
25 resolution of 0.5×0.5 degrees were also used to calculate glacier mass balance.

26 **2.5 Climatic glacier mass balance model**

27 The climatic glacier mass balance model, based on the heat balance method provided by
28 Fujita and Ageta (2000), Fujita et al. (2007), and Fujita et al. (2011), was used to calculate
29 mass balance at all three median elevation categories (G-, L-, and W-average elevations),

1 which are the area-weighted average at each 0.5×0.5 degree grid. Daily heat balance at
 2 glacier surface can be calculated using the following: required air temperature, relative
 3 humidity, wind speed, solar radiation, and precipitation, and mass balance consisting of snow
 4 accumulation, melt, refreezing, and evaporation, such that

$$5 \quad Q_M = (1 - \alpha)R_S + R_L - \sigma T_S^4 + Q_S + E_V l_e + Q_G . \quad (2)$$

6
 7 Q_M , α , R_S , R_L , σ , T_S , Q_S , $E_V l_e$, l_e , and Q_G are heat for melting, surface albedo, downward
 8 shortwave radiation, downward longwave radiation, the Stefan-Boltzmann constant, surface
 9 temperature in Kelvin, sensible heat flux, latent heat flux, latent heat for evaporation of water
 10 or ice and conductive heat flux into the glacier ice, respectively. All heat components are
 11 positive when fluxes are directed toward the surface. Longwave radiation was calculated by
 12 application of the equation established by Kondo and Xu (1997) using dew point temperature
 13 at the screen height and a coefficient related to the sunshine ratio (ratio of downward
 14 shortwave radiation to solar radiation at the top of the atmosphere). The surface temperature is
 15 obtained to satisfy all heat balance equations by iterative calculation of conductive heat. Mass
 16 balance (M_b) on the glacier is calculated as follows:

$$17 \quad M_b = C_a - Q_M/l_m + E_V + R_F \quad (3)$$

18 C_a , l_m , E_V , and R_F are solid precipitation, latent heat for melting ice, condensation (if E_V
 19 has negative value, it is evaporation), and refreezing, respectively. This climatic mass balance
 20 model also takes into account refreezing amounts from ice temperature change, as shown in
 21 Eqn. (2). Calculation interval was daily.

22 The phase of precipitation, solid (snow) (C_a , positive sign) or liquid (rain), depending on
 23 air temperature, is important for glacier mass balance. Precipitation (P_p) is separated solid and
 24 liquid by temperature, assuming the occurrence probability of solid precipitation. The
 25 following relation between the probability of snowfall and air temperature was obtained from
 26 data observed by Fujita and Nuimura (2011) on the Tibetan Plateau:

$$\begin{aligned} C_a &\cong \mathcal{P}_p && [T_a \leq 0] \text{ (}^\circ\text{C)} && (4) \\ &= \left(1 - \frac{T_a}{T_l} \right) P_p && [0 < T_a < T_l] \text{ (}^\circ\text{C)} \text{ and} \\ &= 0 && [T_a \geq T_l] \text{ (}^\circ\text{C)} \end{aligned}$$

1 Here, T_l is the temperature at which all precipitation becomes liquid (rain), which was
2 assumed to be 4 °C. First, we calculated the mass balance at each average elevation using
3 APHRODITE and reanalysis ERA-Interim data from 1979 to 2007, assuming that the initial
4 values of ice temperature and snow depth are annual mean temperature and 0.1 m,
5 respectively. The ice temperature was set to 0 °C when the annual mean exceeded the melting
6 point. Then, we could obtain initial condition values of ice temperature and snow depth for
7 subsequent mass balance calculations from 1979 to 2007. To calculate optimized precipitation
8 at average elevations (P_{cal}), we calculated, assuming that mass balance from 1979 to 2007
9 should be equal to zero by adjusting the APHRODITE precipitation data (P_{ap}) as shown in
10 Fig. 4,

$$11 \quad P_{cal} = A_p \times P_{ap}, \quad (5)$$

12 where A_p is the adjusting ratio of APHRODITE precipitation and A_p is constant for each grid.
13 Both P_{cal} and P_{ap} , include all phases of precipitation (i.e., liquid and solid precipitation) in
14 Eqn. (5). Separated solid precipitation contribute to glacier mass balance. If a snow layer is on
15 the glacier ice, and if the temperature of the snow-covered ice layer is lower than 0°C, some
16 amount of rain (liquid precipitation) and meltwater will refreeze on the ice layer, and that
17 amount corresponds with the heat of the increasing ice temperature. The refrozen ice also
18 contributes to the mass balance of the glacier. If no snow layer on the glacier surface, or if the
19 ice has a 0°C temperature, liquid precipitation and meltwater will be released as discharge,
20 and the discharge does not contribute to the mass balance of the glacier.

21

22 **3 Results**

23 **3.1 Distribution of average elevations of glaciers**

24 Figure 5 shows the distribution of three types of average elevations of glaciers (G-, L-, W-
25 average elevations). The G-average elevations have 951 grid points and the L- and W-average
26 elevations have 670 grids. Several grid cells at the eastern Sayan Mountains, in the west of the
27 Altai Mountains, at the Qilian Mountains, and in the east of Hengduan Shan (see location in
28 Fig. 1) in Fig. 5a (G-average elevation) have been excluded in Fig. 5b (L-average elevation)
29 because those glaciers are smaller than 1 km² in area.

1 Distribution of the difference between W-average elevation and L-average elevation (Fig.
2 S3) indicates that the Tibetan Plateau has less difference. The Kalakoram, the Himalaya, and
3 the Hengduan Shan have relatively large differences, which reflect that glaciers in these
4 regions are surrounded by steep avalanche walls at the upper part. The relation between G-
5 and L-average elevations (Fig. S4) indicates that median elevations changed both positively
6 and negatively by eliminating small size glaciers ($< 1 \text{ km}^2$).

7 In contrast, average elevation of glaciers shift to higher altitude by taking into account
8 steep avalanche walls, which are depicted by the relation between G- and W-average
9 elevations. Furthermore, the change of average elevation of glaciers between G- and L-
10 average is much larger than that between G- and W-average.

11 **3.2 Precipitation contributing to mass balance at ELA**

12 Figure 6 shows that annual precipitation of APHRODITE and calculated precipitations
13 (P_{cal} in Eqn. 5) at average elevation derived from the G-, L-, W-average elevations (Fig. 5).
14 Here these calculated precipitation amounts, which contribute to glacier mass at the G-, L-,
15 W-average elevations, are indicated by P_G , P_L , and P_W , respectively. Little precipitation
16 around the Taklimakan Desert and much precipitation at the Hengduan Shan and the southern
17 edge of the western Himalayas, the Hindu Kush and the Hissar Alay were found. These
18 calculated precipitations at ELA reflect regional climate in High Mountain Asia. Furthermore,
19 they might include inconsistency between average elevation of glaciers and ELA. However,
20 several grids have extraordinarily large amounts of precipitation in the eastern Sayan
21 Mountains, the west of the Altai Mountains, the southern edge of the Himalayas, and the
22 Hengduan Shan (Fig. 6b). Although P_L in Fig. 6c in several grids at the Hengduan Shan, the
23 southern edge of the Himalayas, and the Karakoram was still extremely large, those grids
24 have less P_W in Fig. 6d. Figure S5 shows the difference of P_L to P_W . The difference implies
25 the amount of avalanche nourish contribution. A difference of more than 500 mm is found at
26 high relief terrains, such as the Central and East Himalayas, the Hengduan Shan, the
27 Karakoram, and the Hissar Alay. Then, large amounts of avalanche nourishment would
28 contribute to the glacier mass in those regions. Still, several grids have extremely large
29 precipitation compared with adjacent grids. Those overestimations would be caused by
30 missed glacier delineation or unreasonable estimation of the steep avalanche wall.

31

1 3.3 Evaluation

2 Although direct observations of precipitation at ELA are scarce, winter balance was
3 observed at several glaciers in High Mountain Asia, which was compiled by Dyurgerov
4 (2002) (Table S3). We compared the snow amounts calculated from 1979 to 2000 at the G-,
5 L-, and W-average elevations with observed winter balances, using the value from the
6 corresponding grid cell (Fig. 7) (Table S4). APHRODITE snow was calculated by use of
7 daily temperature at each ELA based on Eqn. (4). The figure shows APHRODITE snow is
8 significantly less than the observed winter accumulation. Furthermore, snow amount derived
9 from G-, L-, and W-average elevations tend to be smaller than the winter balance, but the
10 correlation coefficient is statistically significant and much higher than that with APHRODITE
11 snow.

12 Accumulated snow at the end of winter is reported as “winter balance” in the report of
13 Dyurgerov (2002). The highest correlation coefficient between average observed winter
14 balance and accumulation calculated on the basis of L-average elevation are obtained,
15 although the correlation coefficient between observed winter balance and calculated
16 precipitation based on W-average elevation was low. The reason behind this finding might be
17 the fact that observed winter balance includes not only surface precipitation but also
18 avalanche nourishment during winter. Then, observed winter balance can be a validation for
19 accumulation during winter, including drifting snow and avalanche. However, it cannot be a
20 validation for direct precipitation during winter.

21 We also plotted errors of calculated snow amount caused by input parameters,
22 temperature, T_l in Eqn. (4), solar radiation, and average elevation (Fig. S6). Ranges of air
23 temperature (± 0.9 °C) and solar radiation (± 102 W m⁻²) were from RMSEs between
24 observed data and ERA-Interim data during the summer (JJA), as shown in Fig. S2. The range
25 of T_l was taken as ± 2 °C, the source of which is described in the next section. The range of
26 average elevations comes from the RMSE between observed ELA and average elevation, as
27 shown in Fig. 2. Fig. S6 shows that error of calculated snow caused by solar radiation was the
28 largest parameter among those input parameters.

29

1 **4 Discussion**

2 **4.1 Index of median elevation of glaciers**

3 **4.1.1 Bias of median elevation derived from GAMDAM glacier inventory**

4 In the GGI, we excluded steep slope areas, where snow cannot accumulate, from the
5 glacier area (Nuimura et al., 2014). Then, median elevation derived from the GGI would have
6 lower elevations than those based on glacier inventory that included steep head walls.
7 Bajracharya and Shrestha (2011) created the ICIMOD inventory covering the Hindu Kush-
8 Himalayan (HKH) region (Amudarya, Indus, Ganges, Brahmaputra, and Irrawaddy river
9 basins). This inventory was generated semi-automatically using more than 200 Landsat 7
10 ETM+ images taken between 2002 and 2008. Nuimura et al. (2014) compared median
11 elevations averaged at each grid cell by area-weighting of our GGI and ICIMOD glacier
12 inventory in the HKH region (Fig. 14c in Nuimura et al., 2014). Mean average elevations
13 based on the GGI was 34 m lower than those of ICIMOD glacier inventory in the HKH region.
14 This difference is within the RMSE (71 m) between median elevation and observed ELA.
15 Regional distribution of average elevation difference between the ICIMOD inventory and the
16 GGI are especially large in the Pamir range (approximately 300 m) (Fig. 15c in Nuimura et
17 al., 2014). Then, estimated precipitation by use of G- L- average elevation in the Pamir range
18 would be overestimated.

19

20 **4.1.2 Potential bias of median elevation and W-average elevation**

21 We assumed that median elevation of glaciers correspond with the multi-decadal average
22 of ELA on the basis of Fig. 2. However, the observed glaciers are only nine, with limited
23 observed periods. Then, we have to consider the discrepancy between ELA and median
24 elevation of glaciers in each region. Scherler et al. (2011) reported on regional AARs at high
25 Asian mountains, which estimated the snow line altitude by use of satellite images acquired
26 near the end of the hydrological year. They summarized that glaciers in the Karakoram,
27 northern central Himalayas, and West Kunlun Shan have larger AARs (>0.5). Then, we can
28 estimate that median elevations (i.e., $AAR = 0.5$) of those glaciers correspond to elevations
29 with positive mass balance, which suggests that calculated precipitation at median elevation
30 would be underestimated. Glaciers in the Hindu Kush, western Himalayas, and southern

1 central Himalayas have less AAR (<0.5) according to Scherler et al. (2011), which indicates
2 that the median elevation of those glaciers correspond to the elevations with negative mass
3 balance. Then, calculated precipitations at median elevations in those regions would be
4 overestimated.

5 We estimate W-average elevation by assuming that the maximum altitude of the ground in
6 the grid cell corresponds to the highest altitude of glacier basins. For a more ideal estimation
7 of W-average elevation, we should calculate them at every basin, not every grid cell. Because
8 mountain peaks at glacier headwalls sometimes sort out different grid cells from those
9 glaciers. Those missed segmentations of glaciers and mountain peaks would lead to
10 under/over-estimation of W-average elevation. For example, grid B (Fig. 12) with extremely
11 large A_p would be explained by under estimation of W-average elevation by those missed
12 segmentations (see details in Section 4.3).

13

14 **4.2 Climate on average elevation of glaciers**

15 **4.2.1 Relation between temperature and precipitation at average** 16 **elevation**

17 Several researchers have analysed the relation between summer (JJA) temperature and
18 annual precipitation at ELA (T-P plot) and discussed climatology of glaciers (e.g., Nesje and
19 Dahl, 2000). Ohmura et al. (1992) established the relation between summer (JJA) temperature
20 and annual precipitation at ELA (T-P plot) for 70 glaciers in the world. Braithwaite et al.
21 (2006) also discussed the effect of vertical lapse rate for temperature based on the observed
22 winter balance and model annual temperature sum of 180 glaciers in the world. T-P plots can
23 show the climate regime of glaciers, and the slope of the T-P can indicate the sensitivity of
24 glaciers to temperature change (Ohmura et al., 1992).

25 The T-P plot in Fig. 8 indicates that APHRODITE precipitation cannot represent the
26 relation reported by Ohmura et al. (1992). We also depict T-P plots at G-, L-, W-average
27 elevations at each grid in Fig. 8. T-P plot of G-average elevation includes high temperature
28 range (5° – 10° C). The reason for this finding is that G-average elevation reflects the elevation
29 of small glaciers composed by drifting snow at several tens of grids. T-P plots of L-average
30 elevations contain very large precipitation at the 3° – 5° C temperature range, because glacier

1 mass is affected by avalanche, particularly in the Hengduan Shan, the Himalayas, and the
2 Karakoram. Those fitted curves of G and L have larger inclination than Ohmura's equation at
3 the high temperature range. On the other hand, the fitted curve of the T-P plot based on W-
4 average elevation corresponds well with Ohmura's equation, which implies that calculated
5 precipitation based on W-average elevation represents reasonable results.

6 The T-P plot with error are shown in Fig. S7. Error was derived from RMSE of 71 m
7 between the decadal average of ELA and the median elevation of each glacier (Fig. 2). Then,
8 both vertical and horizontal error bars were calculated, assuming that L-average elevation has
9 a ± 71 m error. Errors on median elevation increase with precipitation. Those tendencies can
10 also be found in the precipitation calculated by use of G- and W-average elevations. We did
11 not show those errors in the figure.

12

13 **4.2.2 Error of calculated precipitation caused by input data**

14 We have not only calculated precipitation errors on median elevation but also have several
15 possible errors of the calculated precipitation at average elevation because of other input data.
16 We assumed that annual air temperature and solar radiation have errors of RMSE between
17 observation and reanalysis data. The temperature at which the probability of solid
18 precipitation becomes 100% is approximately 0 °C. On the other hand, the critical temperature
19 at which the probability of solid precipitation becomes 0% has a wide range, between 3 and 7
20 °C, according to previous research at the Tibetan Plateau (Ueno et al., 1994), Nepal
21 Himalayas (Ageta and Higuchi, 1984), and Qilian Shan (Sakai et al., 2006). The temperature
22 at which all precipitation becomes liquid (T_l) was assumed to be 4 °C in Eqn.(4). Here, we
23 assumed that the critical temperature for all precipitation becoming solid was fixed at 0 °C,
24 and T_l has a range between 2 and 6 (± 2 °C). Then, we calculated each error of precipitation at
25 L-average elevation at each grid cell, and plotted each error of precipitation against P_L in
26 Figure S8.

27 All errors have a large variation against P_L and tend to increase with P_L . Both errors of P_L
28 on input reanalysis data, air temperature, and solar radiation were larger than those of P_L on T_l
29 and average elevation. Then, highly accurate reanalysis data provided in the future will
30 greatly improve the accuracy of estimated precipitation at average elevation.

1

2 **4.2.3 Accumulation season and T-P plot**

3 Fujita (2008a, 2008b) reported that summer-accumulation type glaciers (SAG) have
4 higher sensitivity at ELA under the idealized meteorological variables. Hengduan Shan,
5 Bhutan, Everest, and West Nepal are strongly influenced by the Indian and Southeast Asian
6 summer monsoons, and glaciers are SAG. On the other hand, the climate at Pamir, Hindu
7 Kush, and Karakoram are dominated by the Westerlies, and glaciers are winter-accumulation
8 type glaciers (WAG) (Bookhagen and Burbank, 2010). Himachal Pradesh and Jammu
9 Kashmir (included in the W Himalaya in Fig. 1) are transition zones, influenced by both the
10 monsoon and the Westerlies (Bookhagen and Burbank, 2010). We can classify glaciers into
11 SAG and WAG using the 40% summer (JJA) precipitation ratio (SPR) to annual precipitation
12 (APHRODITE from 1979 to 2007) in High Mountain Asia, as shown in Fig. 9.

13 Sensitivity of the glacier mass can be evaluated by the gradient of the relation between
14 JJA temperature and annual precipitation at ELA (T-P plot), according to Ohmura et al.
15 (1992). Figure 10 shows the T-P plot reported by Ohmura et al. (1992) based on 70 glaciers in
16 the world and calculated at each grid in High Mountain Asia at W-average elevations, which
17 are classified into WAG and SAG. SAG have higher sensitivity than Ohmura's equation,
18 particularly in the high temperature regions. WAG have similar sensitivity with Ohmura's
19 equation. The reason for this finding is that Ohmura et al. (1992) established the P-T plot
20 based mainly on WAG. Plots of SAG have wider variations against the fitted curve than those
21 of WAG (Fig. 10), which reflects that SAG have a wider range distribution in latitude (In
22 other words, SAG have a wider range of summer radiation (Ohmura et al., 1992) than that of
23 WAG (Fig. 10).

24 Braithwaite et al. (2006) also depict the T-P plot on the basis of 180 glaciers, and indicate
25 that Arctic glaciers have low (less than 0°) temperature and less precipitation. Figure 10 also
26 indicates glaciers with less precipitation and low temperature in High Mountain Asia, and
27 those glaciers have less sensitivity to temperature change because high Asian mountains
28 contain glaciers in inland arid regions. Thus, High Mountain Asia can retain the ice mass
29 stably, like glaciers in the Arctic.

30 As described above, seasonal change of precipitation is one of the important factors for
31 mass balance in glaciers. We have analysed seasonal contribution of precipitation from

1 APHRODITE (Fig. S9) to examine the differences among them derived from HAR
2 (Maussion et al., 2014). The main differences of seasonal contribution between HAR and
3 APHRODITE are West Kunlun in JJA and MAM and Karakoram in DJF. According to
4 Yatagai et al. (2012) (Fig. 1), gauge stations contributed to APHRODITE in the Karakoram,
5 but very few contributed at Kunlun. Therefore, the reliability of APHRODITE data is high at
6 Karakoram but less in the Kunlun. Glaciers in the Kunlun Shan have not been classified as
7 SAG on the basis of the HAR provided by Maussion et al. (2014). Less precipitation
8 contribution during MAM and much more during JJA in the Kunlun Shan based on the
9 APHRODITE might have caused a large discrepancy in the calculated precipitation at average
10 elevations, because MAM (spring) accumulation is important for many glaciers in High
11 Mountain Asia (Yang et al., 2013; Maussion et al., 2014). Furthermore, Maussion et al.
12 (2014) found high variability of precipitation seasonality along the central and east Himalayas.
13 We could not find such a high variability of precipitation seasonality in the APHRODITE
14 products because of their coarse resolution. Such discrepancy in precipitation seasonality
15 might cause errors in calculated precipitation.

16

17 **4.2.4 Annual temperature range**

18 We classified glaciers in High Mountain Asia by annual temperature range, which are
19 calculated on the basis of monthly temperature (Fig. 11a). Low annual temperature range (10
20 $< T_r < 20$) area expands to Hengduan Shan, Himalayas, West Kunlun, and Tien Shan. We
21 made a T-P plot for different annual temperature ranges in Fig. 11b, as analysed by
22 Braithwaite (2008). Glaciers with low annual temperature range have higher gradient of T-P
23 plot, which means that those glaciers have higher sensitivity to climate (temperature and
24 precipitation) changes, which is the same result as with Braithwaite (2008). Glaciers with
25 high annual temperature range ($20 < T_r < 30$), which have less sensitivity to climate change,
26 distribute to Sayan, Altai, the Tibetan Plateau, Karakoram, Hindu Kush, and Pamir. Those
27 regions, except Sayan, Altai, and Hindu Kush, correspond to slight mass gain areas (Gardner
28 et al., 2013). They have less sensitivity to climate change because high annual temperature
29 range might be one of the reasons for recent glacier mass gain in these regions.

30

1 4.3 Adjustment ratio of precipitation: A_p

2 Figure 12 shows the distribution of A_p (adjustment ratio of APHRODITE data), calculated
3 on the basis of W-average elevation. Although, W-average elevation at most grids is higher
4 than the elevation in the grid average (including glacier-free zones), the eastern Himalayas,
5 the central Himalayas, Pamir, Karakoram, and central Tien Shan have adjustment ratios of
6 less than 1, implying that the APHRODITE precipitation data overestimate the precipitation
7 at the average elevation of glaciers.

8 We compared the altitudinal distributions of grid numbers for the average elevation of
9 glaciers and the mean altitude of each grid in the Himalayas and the Karakoram (Fig. S10a
10 and S10b). Both modes of average elevation of glaciers and mean altitude of grids show
11 similar altitude (5000 m a.s.l and 5500ma.s.l., respectively). On the other hand, in the
12 Himalayan region, several researchers reported that maximum precipitation occurs at 3000 m
13 elevation (Burbank et al., 2003; Putkonen, 2004; Bookhargen and Burbank, 2006), which is
14 lower than the W-average elevation of glaciers (Fig. S10a). Then, the calculated precipitation
15 at the average elevation of glaciers would be much less than the grid average precipitation (<
16 0.6), which is also affected by larger precipitation at lower elevation because precipitation
17 gauges are usually set at low elevation. Hence, almost all grid cells have less than 0.6 in A_p
18 (Fig. S10c). Fujita and Nuimura (2011) and Fujita and Sakai (2014) also reported that
19 observed precipitation at Tsho Rolpa in the east Nepal Himalayas (27.9 °N, 86.5 °E) was less
20 than the APHRODITE precipitation data. In the Karakoram region, most grid cells have A_p
21 close to 1 (0.4–1.0) in Fig. S10c. The reason is that glaciers in the Karakoram have almost the
22 same altitudinal distribution of W-average glacier elevation and average ground altitude, at
23 which the altitude of peak precipitation (5000–6000 m a.s.l.) corresponded (Wake, 1989;
24 Young and Schmok, 1989; Young and Hewitt, 1990; Hewitt, 2011).

25 Yatagai et al. (2012) compared the APHRODITE with the Global Precipitation
26 Climatology Centre (GPCC) product, which is also compiled gauge precipitation data.
27 Distribution of the difference (APHRODITE-GPCC) (Fig. 9a of Yatagai et al., 2012)
28 indicates that APHRODITE estimates less precipitation than the GPCC product in most areas.
29 APHRODITE data, however, were larger than the GPCC product only around the central Tien
30 Shan and Pamir regions. Then, those regions have the adjustment ratio of less than 1.

31 Three grids have extremely large A_p (>10), indicated by A–C in Fig. 12. The reason A
32 (48.5°–49.0°N, 89.0°–89.5°E) and C (28.0°–28.5°N, 93.0°–93.5°E) have large A_p can be

1 explained by missed delineation of glacier area. Glaciers in the shadow at the upper part of the
2 glacier area are excluded in grid A and some snow patches at the top of the mountain ridges
3 are included in error in grid C. In grid B (36.0°–36.5°N, 74.5°–75.0°E), the upper part of the
4 glaciers in the GGI are excluded and furthermore, a high mountain peak is located north of
5 the grid, and glaciers flow down from the peak. In the calculation of W-average elevation,
6 other relatively low-peak mountains are applied for maximum altitude of ground. Then the
7 W-average elevation is underestimated.

8

9 **5 Conclusion**

10 We calculated precipitation at median elevation by assuming that median elevation
11 coincides with ELA, using a climatic glacier mass balance model by adjusting precipitation
12 data. Three types of average elevations of glaciers are proposed. They are (1) G-average
13 elevation, which includes small glaciers ($< 1 \text{ km}^2$), (2) L-average elevation, which eliminates
14 small glaciers, and (3) W-average elevation, which is calculated to include steep avalanche
15 walls. L-average elevation eliminated local terrain effects, such as drifting snow, which was
16 included in G-average elevation. W-average elevation depends only on climate and excludes
17 the effect of avalanche nourishment.

18 Precipitation estimated based on G- and L-average elevation have extremely large values
19 at several tens of grids, and those fitted curves of T-P plots have large gradients. In contrast,
20 distribution of precipitation calculated on the basis of W-average elevation reduces the
21 number of extremely large amounts of precipitation, because the W-average glacier elevation
22 depends only on climate and is not affected by avalanche nourishment.

23 Estimated precipitation at W-average elevations elucidated the T-P conditions of glaciers
24 in High Mountain Asia. Glaciers in High Mountain Asia are located in low temperature zones,
25 like glaciers in the Arctic. Furthermore, it was elucidated that glaciers in high relief terrains
26 (such as the central and eastern Himalayas and the Hengduan Shan, the Karakoram, and the
27 Pamir) tend to have large amounts of avalanche nourishment contribution to the glacier mass by
28 comparing P_L (including avalanche nourishment) and P_W (only direct precipitation).

29 We differentiated summer-accumulation type glaciers and winter-accumulation type
30 glaciers using the 40% summer precipitation ratio to annual precipitation. Fitted curves of
31 winter-accumulation type glaciers corresponded well with Ohmura's equation. However, the

1 curves of summer-accumulation type glaciers have higher gradients, particularly at larger
2 precipitation ranges, which indicate that summer-accumulation type glaciers have higher
3 sensitivity to climate change. P-T plots classified by high and low annual temperature ranges
4 clarified that glaciers with high annual temperature range have lower sensitivity to climate
5 change, as indicated by Braithwaite (2008). Furthermore, low sensitivity to climate change
6 because of high annual temperature range might be one of the reasons for recent slight mass
7 gain in glaciers in Karakoram, Pamir, and the Tibetan Plateau reported by Gardner et al.
8 (2013).

9 A_p values were much less than 1 at the western, central, and eastern Himalayas, and
10 approximately 1 at Karakoram. The reason for this finding is the altitudinal relation between
11 the average elevation of glaciers and the precipitation gradient.

12 In future studies, the estimated precipitation in High Mountain Asia will possibly reveal
13 precise sensitivity of glaciers to climate change, and they will provide proper contribution of
14 glacier runoff in High Mountain Asia.

15

16 **Acknowledgements**

17 We thank T. Bolch, R. Braithwaite, and an anonymous reviewer for their valuable comments.
18 This research was supported by the Funding Program for Next Generation World-Leading
19 Researchers (NEXT Program). We express our sincere thanks and appreciation for great
20 support to Mrs. Y. Hoshina, Dr. S. Tsutaki, Dr. K. Tsunematu, Dr. S. Omiya, Dr. S. Okamoto,
21 Dr. K. Taniguchi, and Mr. P. Tshering.

22

1 **References**

- 2 Adam, J. C., Clark, E. A., Lettenmaier, D. P., and Wood, E. F.: Correction of global
3 precipitation products for orographic effects, *J. Climate*, 19(1), 15-38, 2006.
- 4 Aizen, V. B., Aizen, E. M., Joswiak, D. R., Fujita, K., Takeuchi, N., and Nikitin S. A.:
5 Climatic and atmospheric circulation pattern variability from ice-core
6 isotope/geochemistry records (Altai, Tien Shan and Tibet). *Ann. Glaciol.*, 43, 49-60,
7 2006a.
- 8 Aizen, V. B., Kuzmichenok, V. A., Surazakov, A. B., and Aizen, E. M.: Glacier changes in
9 the central and northern Tien Shan during the last 140 years based on surface and
10 remote-sensing data, *Ann. Glaciol.*, 43, 202-213, 2006b.
- 11 Ageta, Y. and Higuchi, K.: Estimation of mass balance components of summer-accumulation
12 type glacier in the Nepal Himalaya, *Geogr. Ann.*, 66A(3), 249-255, 1984.
- 13 Bajracharya, S. R. and Shrestha, B. (Eds.): The status of glaciers in the Hindu Kush-
14 Himalayan region. International Centre for Integrated Mountain Development
15 Kathmandu. 2011.
- 16 Benn, I. D. and Lehmkuhl, F.: Mass balance and equilibrium-line altitudes of glaciers in high-
17 mountain environments, *Quatern. Int.*, 65/66, 15-29, 2000.
- 18 **Böhner, J.: General climatic controls and topoclimatic variations of Central and High Asia,**
19 ***Boreas*, 35, 279–295, 2006.**
- 20 Bolch, T., Kulkarni, A., Käab, A., Huggel, C., Paul, F., Cogley, J., Frey, H., Kargel, J., Fujita,
21 K., Scheel, M., Bajracharya, S., and Stoffel, M.: The state and fate of Himalayan
22 Glaciers, *Science*, 336, 310–314, doi:10.1126/science.1215828, 2012.
- 23 Bookhagen, B. and Burbank, D. W.: Topography, relief, and TRMM-derived rainfall
24 variations along the Himalaya, *Geophys. Res. Lett.*, 33, L08405,
25 doi:10.1029/2006GL026037. 2006.
- 26 Bookhagen, B. and Burbank, D.: Toward a complete Himalayan hydrological budget:
27 spatiotemporal distribution of snowmelt and rainfall and their impact on river
28 discharge, *J. Geophys. Res.*, 115, F03019, doi:10.1029/2009JF001426, 2010.

- 1 Braithwaite, R. J. and Raper, S. C. B.: Glaciers and their contribution to sea level change,
2 *Phys. Chem. Earth*, 27, 1445–1454, 2002.
- 3 Braithwaite, R. J. and Raper, S. C. B.: Estimating equilibrium-line altitude (ELA) from
4 glacier inventory data, *Ann. Glaciol.*, (50)53, 127-132, 2009.
- 5 Braithwaite, R. J.: Temperature and precipitation climate at the equilibrium-line altitude of
6 glaciers expressed by the degree-day factor for melting snow. *J. Glaciol.*, 54(186),
7 437- 444, 2008.
- 8 Braithwaite, R. J., Raper, S. C. B., and Chutko, K.: Accumulation at the equilibrium-line
9 altitude of glaciers inferred from a degree-day model and tested against field
10 observations, *Ann. Glaciol.*, 43, 329-334, 2006.
- 11 Braithwaite, R. J. and Zhang, Y.: Modelling changes in glacier mass balance that may occur
12 as a result of climate changes, *Geogr. Ann.*, 81A (4), 489-496, 1999.
- 13 Burbank, D. W., Blythe, A. E., Putkonen, J., Pratt-Sitaula, B., Gabet, E., Oskin, M., Barros,
14 A., and Ojha, T. P.: Decoupling of erosion and precipitation in the Himalayas, *Nature*,
15 426(6967), 652-655, <http://dx.doi.org/10.1038/nature02187>, 2003.
- 16 Carrivick, J. L. and Brewer, T. R.: Improving local estimations and regional trends of glacier
17 equilibrium line altitudes, *Geogr. Ann.*, 86A, 67-79, 2004.
- 18 Chen, M. P., Xie, P., Janowiak, J. E., and Arkin, P. A.: Global land precipitation: A 50-yr
19 monthly analysis based on gauge observations. *J. Hydrometeor.*, 3, 249-266, 2002.
- 20 Dahl, S. O. and Nesje, A.: Paleoclimatic implications based on equilibrium-line altitude
21 depressions of reconstructed Younger Dryas and Holocene cirque glaciers in inner
22 Nordfjord, western Norway. *Palaeogeogr. Palaeocl.*, 94, 87-97, 1992.
- 23 Daly, C., Neilson, R. P., and Phillips, D. L.: A statistical–topographic model for mapping
24 climatological precipitation over mountainous terrain, *J. Appl. Meteor.*, 33, 140-158,
25 1994.
- 26 Dee, D. P., Uppala, S. M., Simmons, A. J., Berrisford, P., Poli, P., Kobayashi, S., Andrae, U.,
27 Balsameda, M. A., Balsamo, G., Bauer, P., Bechtold, P., Beljaars, A. C. M., van de
28 Berg, L., Bidlot, J., Bormann, N., Delsol, C., Dragani, R., Fuentes, M., Geer, A. J.,
29 Haimberger, L., Healy, S. B., Hersbach, H., Hólm, E. V., Isaksen, L., Kållberg, P.,
30 Köhler, M., Matricardi, M., McNally, A. P., Monge-Sanz, B. M., Morcrette, J.-J.,

- 1 Park, B.-K., Peubey, C., de Rosnay, P., Tavalato, C., Thépaut, J.-N., and Vitart, F.:
2 The ERA-Interim reanalysis: configuration and performance of the data assimilation
3 system. *Q.J.R. Meteorol. Soc.*, 137: 553–597. doi: 10.1002/qj.828, 2011.
- 4 Dyurgerov, M. B.: Glacier mass balance and regime: Data of measurements and analysis,
5 Occasional Paper 55 (Institute of Arctic and Alpine Research, University of
6 Colorado, Boulder, CO), 2002.
- 7 Engelhardt, M., Schuler, T. V., and Andreassen, L. M.: Evaluation of gridded precipitation for
8 Norway using glacier mass-balance measurements, *Geogr. Ann., Series A, Physical
9 Geography*, 94, 501-509. doi:10.1111/j.1468-0459.2012.00473.x, 2012.
- 10 Fujita, K.: Effect of dust event timing on glacier runoff: sensitivity analysis for a Tibetan
11 glacier, *Hydrol. Process.*, 21(21), 2892-2896, doi:10.1002/hyp.6504, 2007.
- 12 **Fujita, K.: Effect of precipitation seasonality on climatic sensitivity of glacier mass balance,**
13 ***Earth Planet. Sci. Lett.*, 276(1–2), 14–19, doi:10.1016/j.epsl.2008.08.028, 2008a.**
- 14 Fujita, K.: Influence of precipitation seasonality on glacier mass balance and its sensitivity to
15 climate change, *Ann. Glaciol.*, 48, 88-92. doi:10.3189/172756408784700824, 2008b.
- 16 Fujita, K., Seko, K., Ageta, Y., Pu, J. C., and Yao, T. D.: Superimposed ice in glacier mass
17 balance on the Tibetan Plateau, *J. Glaciol.*, 42(142), 454-460, 1996.
- 18 Fujita, K, Ageta, Y., Pu, J., and Yao, T.: Mass balance of Xiao Dongkemadi Glacier on the
19 central Tibetan Plateau from 1989 to 1995. *Ann. Glaciol.*, 31, 159-163, 2000.
- 20 Fujita, K. and Ageta, Y.: Effect of summer accumulation on glacier mass balance on the
21 Tibetan Plateau revealed by mass-balance model, *J. Glaciol.*, 46(153), 244-252, 2000.
- 22 Fujita, K., Ohta, T., and Ageta, Y.: Characteristics and climatic sensitivities of runoff from a
23 cold-type glacier on the Tibetan Plateau, *Hydrol. Process.*, 21(21), 2882-2891,
24 doi:10.1002/hyp.6505, 2007.
- 25 Fujita, K. and Nuimura, T.: Spatially heterogeneous wastage of Himalayan glaciers, *P. Natl.*
26 *Acad. Sci. USA*, 108(34), 14011-14014. doi:10.1073/pnas.1106242108, 2011.
- 27 Fujita, K, Takeuchi, N., Nikitin, S. A., Surazakov, A. B., Okamoto, S., Aizen, V. B., and
28 Kubota, J.: Favorable climatic regime for maintaining the present-day geometry of
29 the Gregoriev Glacier, Inner Tien Shan, *The Cryosphere*, 5(3), 539-549,
30 doi:10.5194/tc-5-539-2011, 2011.

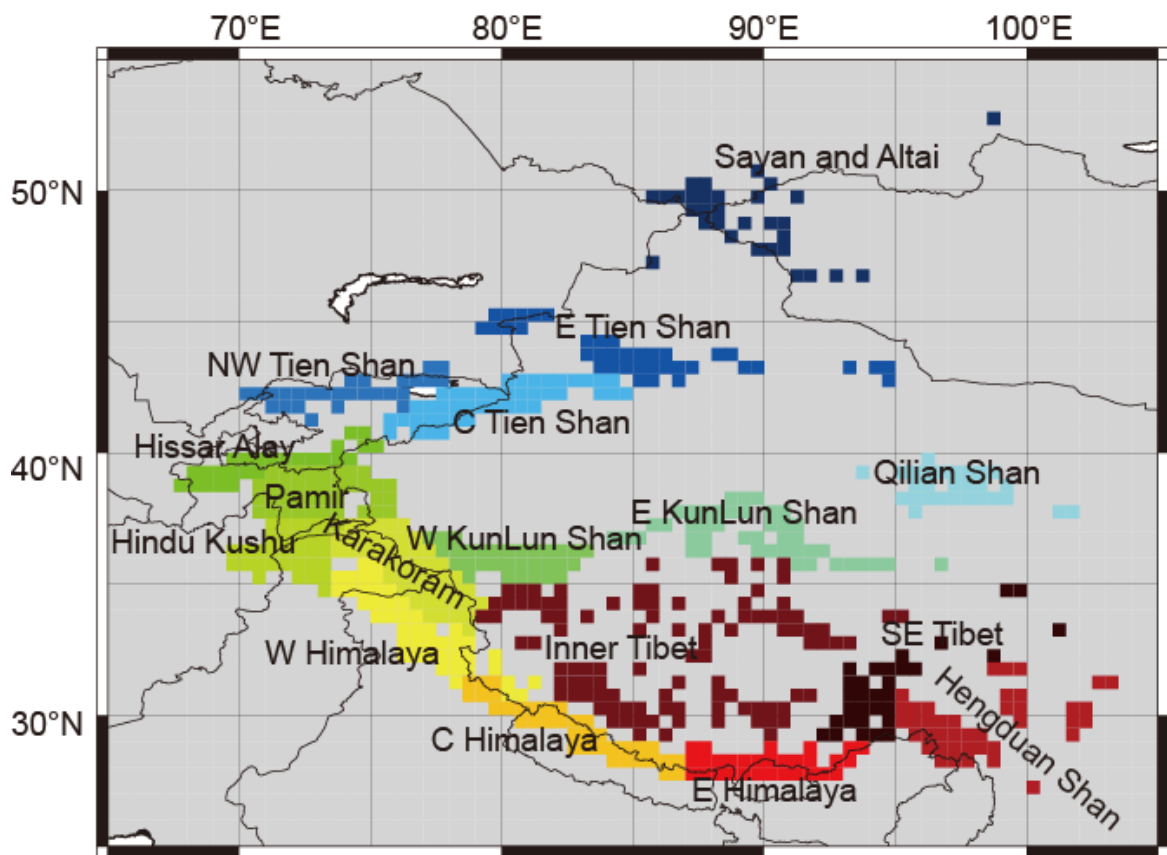
- 1 Fujita, K. and Sakai, A.: Modelling runoff from a Himalayan debris-covered glacier, *Hydrol.*
2 *Earth Syst. Sci. Discuss.*, 11, 2441-2482, doi:10.5194/hessd-11-2441-2014, 2014.
- 3 Gardelle, J., Berthier, E., Arnaud, Y., and Kääb, A.: Region-wide glacier mass balances over
4 the Pamir-Karakoram-Himalaya during 1999–2011, *The Cryosphere*, 7, 1263-1286,
5 doi:10.5194/tc-7-1263-2013, 2013.
- 6 Gardner, A. S., Moholdt, G., Cogley, J. G., Wouters, B., Arendt, A. A., Wahr, J., Berthier, E.,
7 Hock, R., Pfeffer, W. T., Kaser, G., Ligtenberg, S.R.M., Bolch, T., Sharp, M. J.,
8 Hagen, J. O., van den Broeke, M. R., and Paul, F.: A Reconciled Estimate of Glacier
9 Contributions to Sea Level Rise: 2003 to 2009, *Science*, 340 (6134), 852-857,
10 doi:10.1126/science.1234532, 2013.
- 11 Harper, J. T. and Humphrey, N.: High Altitude Himalayan Climate Inferred from Glacial Ice
12 Flux, *Geophys. Res. Lett.*, 30(14), 1764, doi:10.1029/2003GL017329, 2003.
- 13 Hewitt, K.: Glacier change, concentration, and elevation effects in the Karakoram Himalaya,
14 Upper Indus Basin, *Mt. Res. Dev.*, 31(3), 188-200, 2011.
- 15 Hewitt, K.: *Glaciers of the Karakoram Himalaya*. Springer, pp 363. 2014.
- 16 Huffman, G. J., Adler, R. F., Arkin, P., Chang, A., Ferraro, R., Gruber, A., Janowiak, J., and
17 McNab, A.: The Global Precipitation Climatology Project (GPCP) combined
18 precipitation dataset. *Bull. Amer. Meteor. Soc.*, 78, 5-20, 1997.
- 19 Immerzeel, W. W., Ludovicus, P. H. B., and Bierkens, M. F. P.: Climate Change Will Affect
20 the Asian Water Towers, *Science*, 328(5984), 1382-1385,
21 doi:10.1126/science.1183188, 2010.
- 22 Immerzeel, W. W., Pellicciotti, F., and Shrestha, A. B.: Glaciers as a Proxy to Quantify the
23 Spatial Distribution of Precipitation in the Hunza Basin, *Mt. Res. Dev.*, 32(1), 30-38,
24 2012.
- 25 Immerzeel, W. W., Pellicciotti, F., and Bierkens, M. F. P.: Rising river flows throughout the
26 twenty-first century in two Himalayan glacierized watersheds, *Nature Geoscience*,
27 doi:10.1038/NGEO1896, 2013.
- 28 Jaedicke, C. and Gauer, P.: The influence of drifting snow on the location of glaciers on
29 western Spitsbergen, *Svalbard. Ann. Glaciol.*, 42, 237-242, 2005.

- 1 Kääh, A., Teichler, D., Nuth, C. and Berthier, E.: Brief Communication: Contending
2 estimates of 2003–2008 glacier mass balance over the Pamir–Karakoram–Himalaya,
3 *Cryosphere*, 557–564, 2015.
- 4 Kääh, A., Berthier, E., Nuth, C., Gardelle, J., and Arnaud, Y.: Contrasting patterns of early
5 twenty-first-century glacier mass change in the Himalayas, *Nature*,
6 doi:10.1038/nature11324, 2012.
- 7 Kalnay, E., Kanamitsu, M., Kistler, R., Collins, W., Deaven, D., Gandin, L., Iredell, M., Saha,
8 S., White, G., Woollen, J., Zhu, Y., Chelliah, M., Ebisuzaki, W., Higgins, W.,
9 Janowiak, J., Mo, K. C., Ropelewski, C., Wang, J., Leetmaa, A., Reynolds, R., Jenne,
10 R., and Joseph, D.: The NCEP/NCAR 40-year reanalysis project, *B. Am. Meteorol.*
11 *Soc.*, 77(3), 437–471, 1996.
- 12 Kaser, G., Großhauser, M., and Marzeion B.: Contribution potential of glaciers to water
13 availability in different climate regimes, *P. Natl. Acad. Sci. USA*, 107(47), 20223-
14 20227, 2010.
- 15 Kondo J, and Xu J.: Seasonal variations in the heat and water balances for nonvegetated
16 surfaces. *Journal of Appl. Meteor.*, 36, 1676-1695, 1997.
- 17 Maussion, F., Scherer, D. Mölg, T. Collier, E. Curio, J. and Finkelburg R.: Precipitation
18 seasonality and variability over the Tibetan Plateau as resolved by the High Asia
19 Reanalysis, *J. Climate*, 27, 1910-1927, doi:10.1175/JCLI-D-13-00282.1, 2014.
- 20 Narama, C., Kääh, A., Duishonakunov, M. and Abdrakhmatov, K.: Spatial variability of
21 recent glacier area changes in the Tien Shan Mountains, Central Asia, using Corona
22 (1970), Landsat (2000), and ALOS (2007) satellite data, *Global Planet. Change*, 71,
23 42–54, 2010.
- 24 Neckel, N., Kropáček, J., Bolch, T. and Hochschild, V.: Glacier mass changes on the Tibetan
25 Plateau 2003–2009 derived from ICESat laser altimetry measurements,
26 *Environmental Research Letters*, 9, 14009, 2014.
- 27 Nesje, A. and Dahl, S. O.: *Glaciers and environmental change*. London, Arnold. 2000.
- 28 New, M., Hulme, M., and Jones, P.: Representing twentieth century space-time climate
29 variability. I. Development of a 1961–1990 mean monthly terrestrial climatology, *J.*
30 *Climate*, 12, 829-856, 1999.

- 1 New, M., Hulme, M., and Jones, P.: Representing twentieth-century space–time climate
2 variability. Part II: Development of 1961– 90 monthly grids of terrestrial surface
3 climate. *J. Climate*, 13, 2217-2238, 2000.
- 4 Nuimura, T., Sakai, A., Taniguchi, K., Nagai, H., Lamsal, D., Tsutaki, S., Kozawa, A.,
5 Hoshina, Y., Takenaka, S. Omiya, S., Tsunematsu K., Tshering, P., and Fujita, K.:
6 The GAMDAM Glacier Inventory: a quality controlled inventory of Asian glaciers,
7 *The Cryosphere Discuss.*, 8, 1-32, doi:10.5194/tcd-8-1-2014, 2014.
- 8 Oerlemans, J. and Fortuin, J. P. F.: Sensitivity of glaciers and small ice caps to greenhouse
9 warming, *Science*, 258(5079), 115-117, 1992.
- 10 Ohmura, A., Kasser, P., and Funk, M.: Climate at the equilibrium line altitude, *J. Glaciol.*,
11 38(130), 397-411, 1992.
- 12 Paul, F., Kääb, A., Maisch, M., Kellenberger, T., and Haeberli, W.: The new remote-sensing-
13 derived Swiss glacier inventory: I. Methods, *Ann. Glaciol.*, 34, 355-361, 2002.
- 14 Paul, F., Barry, R. G., Cogley, J. G., Frey, H., Haeberli, W., Ohmura, A., Ommanney, C. S. L.,
15 Raup, B., Rivera, A., and Zemp, M.: Recommendations for the compilation of
16 glacier inventory data from digital sources, *Ann. Glaciol.*, 50(53), 119-126, 2009.
- 17 Pfeffer, W. T., Arendt, A. A., Bliss, A., Bolch, T., Cogley, J. G., Gardner, A. S., Hagen, J. O.,
18 Hock, R., Kaser, G., Kienholz, C., Miles, E. S., Moholdt, G., Mölg, N., Paul, F.,
19 Radić, V., Rastner, P., Raup, B. H., Rich, J., and Sharp, M. J.: The Randolph
20 consortium: The Randolph Glacier Inventory: a globally complete inventory of
21 glaciers, *J. Glaciol.*, 60(221), 537-552, 2014.
- 22 Putkonen, J. K.: Continuous snow and rain data at 500 to 4400 m altitude near Annapurna,
23 Nepal, 1991–2001. *Arct. Antarct. Alp. Res.*, 36(2), 244-248,
24 [http://dx.doi.org/10.1657/1523-0430\(2004\)036](http://dx.doi.org/10.1657/1523-0430(2004)036), 2004.
- 25 Racoviteanu, A. E., Arnaud, Y., Williams, M. W., and Ordonez, J.: Decadal changes in
26 glacier parameters in the Cordillera Blanca, Peru, derived from remote sensing, *J.*
27 *Glaciol.*, 54(186), 499-510, 2008.
- 28 Rasmussen, L. A.: Meteorological controls on glacier mass balance in High Asia, *Ann.*
29 *Glaciol.*, 54(63), 352-359, doi:10.3189/2013AoG63A353, 2013.

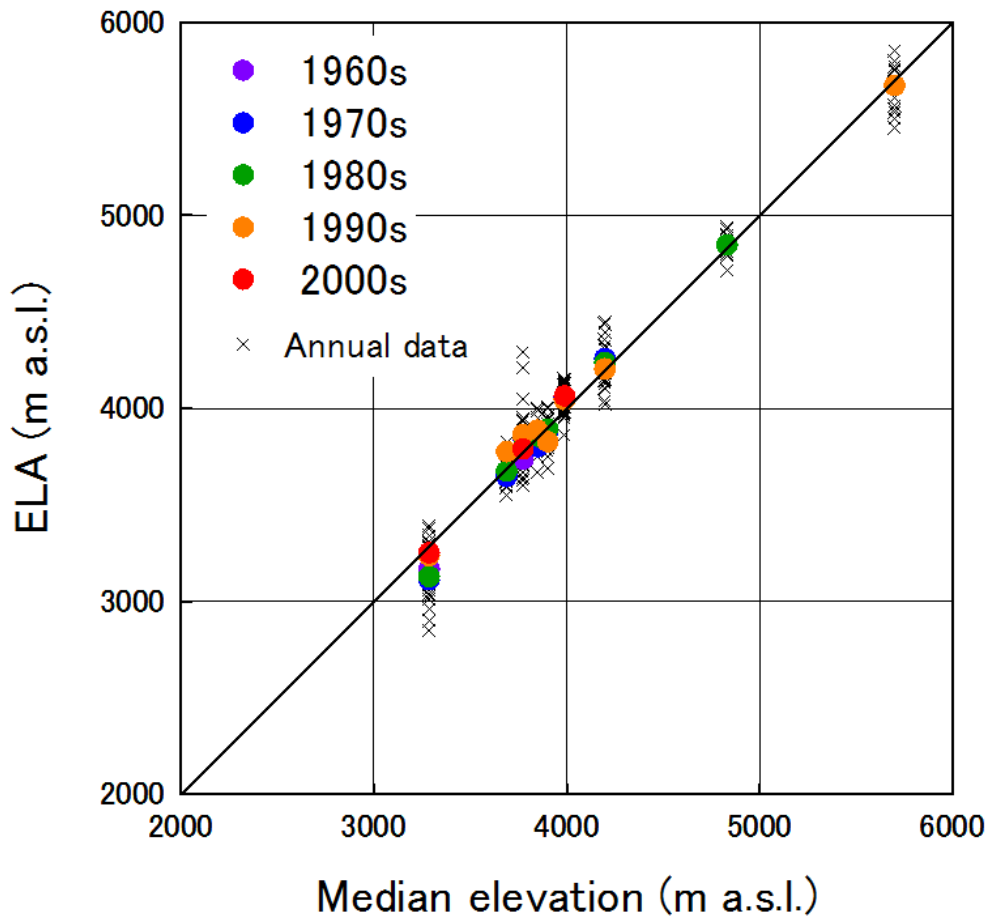
- 1 Rastner, P., Bolch, T., Mölg, N., Machguth, H., Bris, R. L., and Paul, F.: The first complete
2 inventory of the local glaciers and ice caps on Greenland, *The Cryosphere*, 6, 1483-
3 1495, doi:10.5194/tc-6-1483-2012, 2012.
- 4 Rupper, S. and Roe, G.: Glacier changes and regional climate: a mass and energy balance
5 approach, *J. Climate*, 21(20), 5384-5401, doi: 10.1175/2008JCLI2219.1, 2008.
- 6 Sakai A, Matsuda Y, Fujita K, Matoba S, Uetake J, Satow K, Duan K, Pu J, Nakawo M, Yao
7 T.: Meteorological observation at July 1st Glacier in northwest China from 2002 to
8 2005. *Bulletin of Glaciological Research*, 23, 23-31, 2006.
- 9 Sato, T., Tsujimura, M., Yamanaka, T., Iwasaki, H., Sugimoto, A., Sugita, M., Kimura, F.,
10 Davaa, G., and Oyunbaatar, D.: Water sources in semiarid northeast Asia as revealed
11 by field observations and isotope transport model. *J. Geophys. Res.*, 112, D17112,
12 doi:10.1029/2006JD008321, 2007.
- 13 Scherler, D., Bookhagen, B., and Strecker, M. R.: Hillslope glacier coupling: The interplay of
14 topography and glacial dynamics in High Asia, *J. Geophys. Res.*, 116, F02019,
15 doi:10.1029/2010JF001751, 2011.
- 16 Shi, Y. (Eds.): *Concise Glacier Inventory of China*, Shanghai Popular Science Press, China,
17 2008.
- 18 Sorg, A., Bolch, T., Stoffel, M., Solomina, O., and Beniston, M.: Climate change impacts on
19 glaciers and runoff in Tien Shan (Central Asia), *Nature Climate Change*, doi:
20 10.1038/NCLIMATE1592, 2012.
- 21 Surazakov, A. B., Aizen, V. B. Aizen, E. M., and Nikitin S. A.: Glacier changes in the
22 Siberian Altai Mountains, Ob river basin, (1952–2006) estimated with high
23 resolution imagery, *Environ. Res. Lett.*, 2, doi:10.1088/1748-9326/2/4/045017, 2007.
- 24 Torsnes, I., Rye, N., and Nesje, A.: Modern and Little Ice Age equilibrium-line altitudes on
25 outlet valley glaciers from Jostedalbreen, Norway: an evaluation of different
26 approaches to their calculation, *Arctic Alpine Res.*, 25 (2), 106-116, 1993.
- 27 Wake, C. P.: Glaciochemical investigations as a tool to determine the spatial variation of
28 snow accumulation in the Central Karakoram, Northern Pakistan. *Ann. Glaciol.*, 13,
29 279-284, 1989.

- 1 Yang, W., Yao, T., Guo, X., Zhu, M., Li, S., and Kattel, D. B.: Mass balance of a maritime
2 glacier on the southeast Tibetan Plateau and its climatic sensitivity. *J. Geophys. Res.*,
3 118, 9579-9594. doi:10.1002/jgrd.50760, 2013.
- 4 Yao, T., and Coauthors,: Different glacier status with atmospheric circulations in Tibetan
5 Plateau and surroundings, *Nat. Climate Change*, 2, 663–667,
6 doi:10.1038/nclimate1580, 2012.
- 7 Yatagai, A. O., Arakawa, K., Kamiguchi, H., Kawamoto, M., Nodzu, I., and Hamada, A.: A
8 44-year daily gridded precipitation dataset for Asia based on a dense network of rain
9 gauges, *SOLA*, 5, 137-140, doi:10.2151/sola.2009-035, 2009.
- 10 Yatagai, A., Kamiguchi, K., Arakawa, O., Hamada, A., Yasutomi N., and Kitoh, A.:
11 APHRODITE: Constructing a Long-term Daily Gridded Precipitation Dataset for
12 Asia based on a Dense Network of Rain Gauges, *B. Am. Meteorol. Society*,
13 doi:10.1175/BAMS-D-11-00122.1. 2012.
- 14 Yoshimura, K., Oki, T., Ohte, N., and Kanae, S.: Colored Moisture Analysis Estimates of
15 Variations in 1998 Asian Monsoon Water Sources. *Journal of the Meteorological*
16 *Society of Japan*, 82(5), 1315-1329, 2004.
- 17 Young, G. J. and Hewitt, K.: Hydrology research in the upper Indus basin, Karakoram
18 Himalaya, Pakistan, *IAHS Publications*, 190, 139-152, 1990.
- 19 Young, G. J. and Schmok, J. P.: Ice loss in the ablation area of a Himalayan glacier: Studies
20 on Miar Glacier, Karakorum Mountains, Pakistan, *Ann. Glaciol.*, 13, 289-293, 1989.
- 21 Zech, R., Abramowski, U., Glaser, B., Sosin, P., Kubik, P. W., and Zech, W.: Late
22 Quaternary glacial and climate history of the Pamir Mountains derived from
23 cosmogenic ¹⁰Be exposure ages, *Quaternary Res.*, 64, 212 – 220, 2005.
- 24



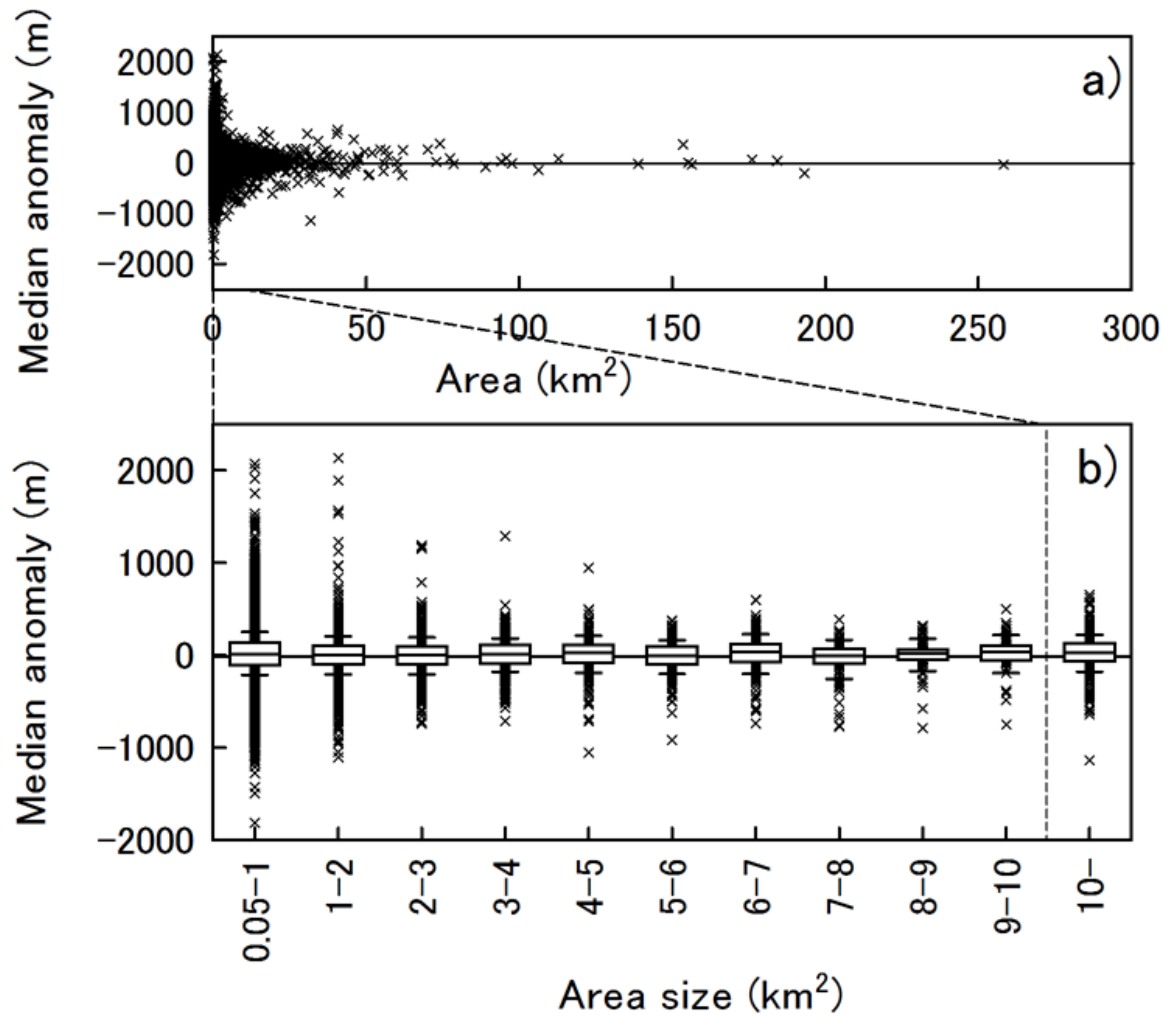
1
2
3
4
5
6

Fig. 1. Study area: High Mountain Asia. Region name and location of the grid that the GGI occupied.



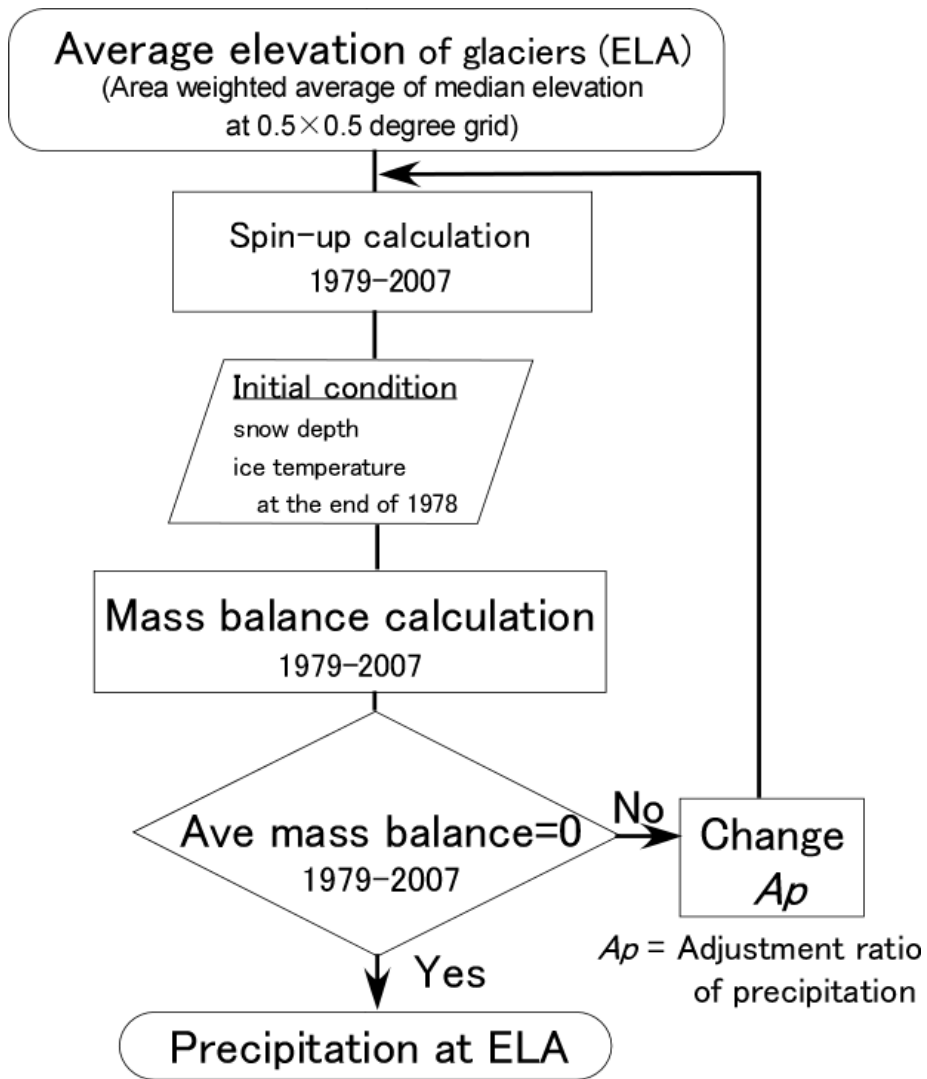
1
2
3
4
5
6

Fig. 2. Relation between median elevation derived from the GGI and annual observed ELAs (cross marks) and decadal average of observed ELA (coloured circles) on nine glaciers in High Mountain Asia.



1
2
3
4
5
6
7

Fig. 3. (a) Relation between glacier area and median anomaly, which has glaciers with more than 300 vicinity glaciers (within 0.5×0.5 degree grid). (b) Median anomaly distribution in 1-km^2 bins up to 10 km^2 . Boxes give lower and upper quartiles of median glacier altitude in 1-km^2 bin. Vertical error bars indicate standard deviation of data range. Crosses lie outside of this range.

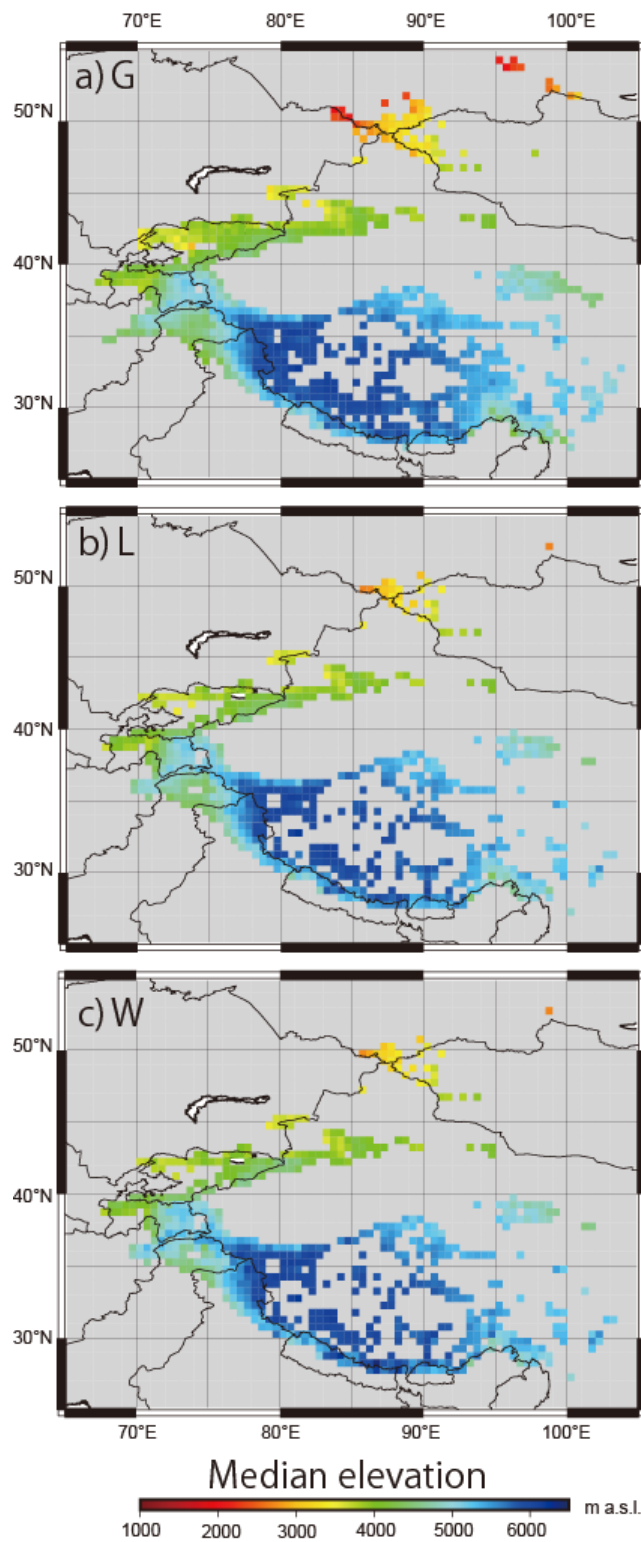


1

2 Fig. 4. Flowchart of calculation of precipitation at average elevation of glaciers.

3

4

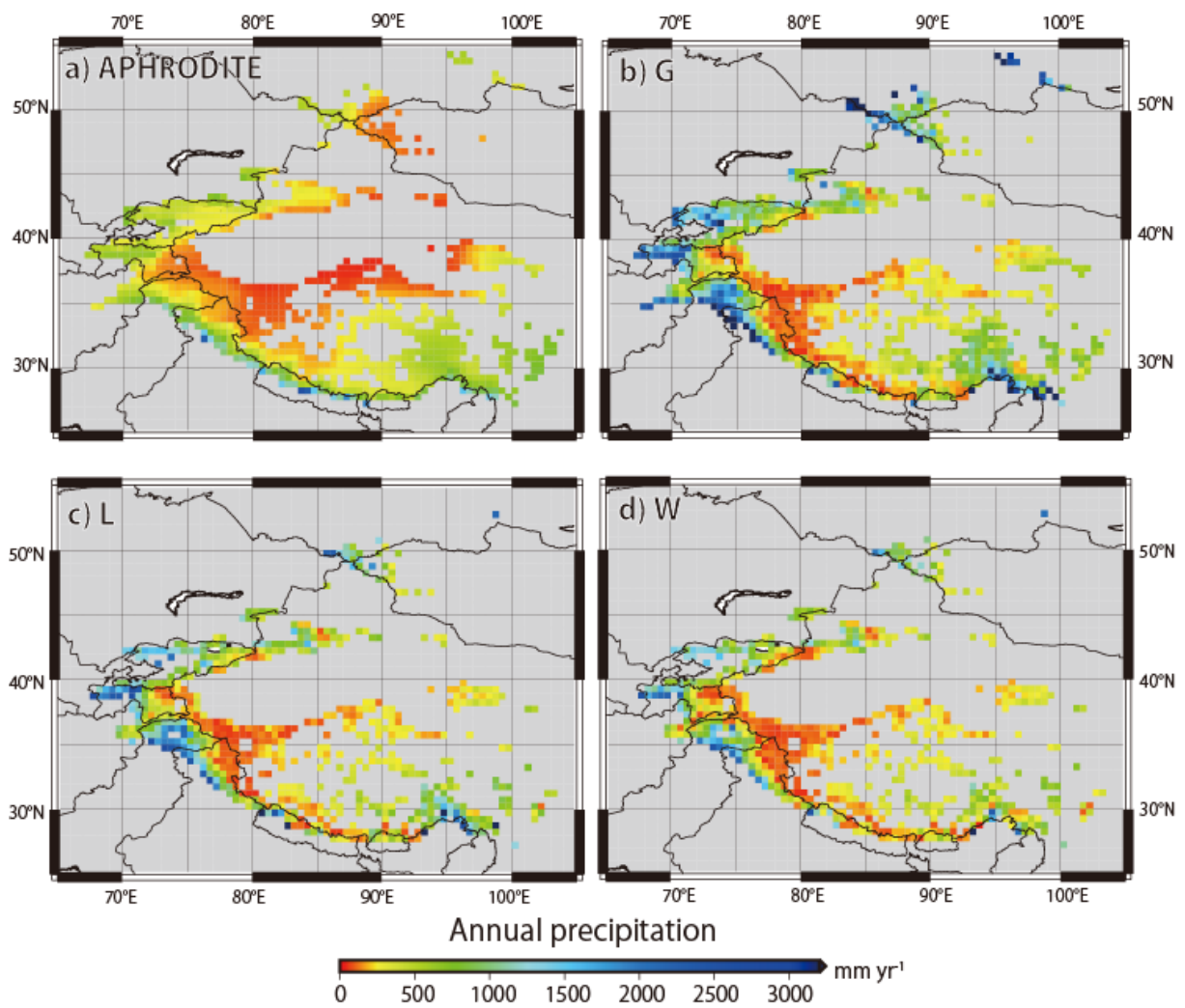


1

2 Fig. 5. Distributions of (a) G-, (b) L-, and (c) W-average elevation. These distributions are the
 3 area-weighted average of median elevations at each 0.5 degree grid.

4

5

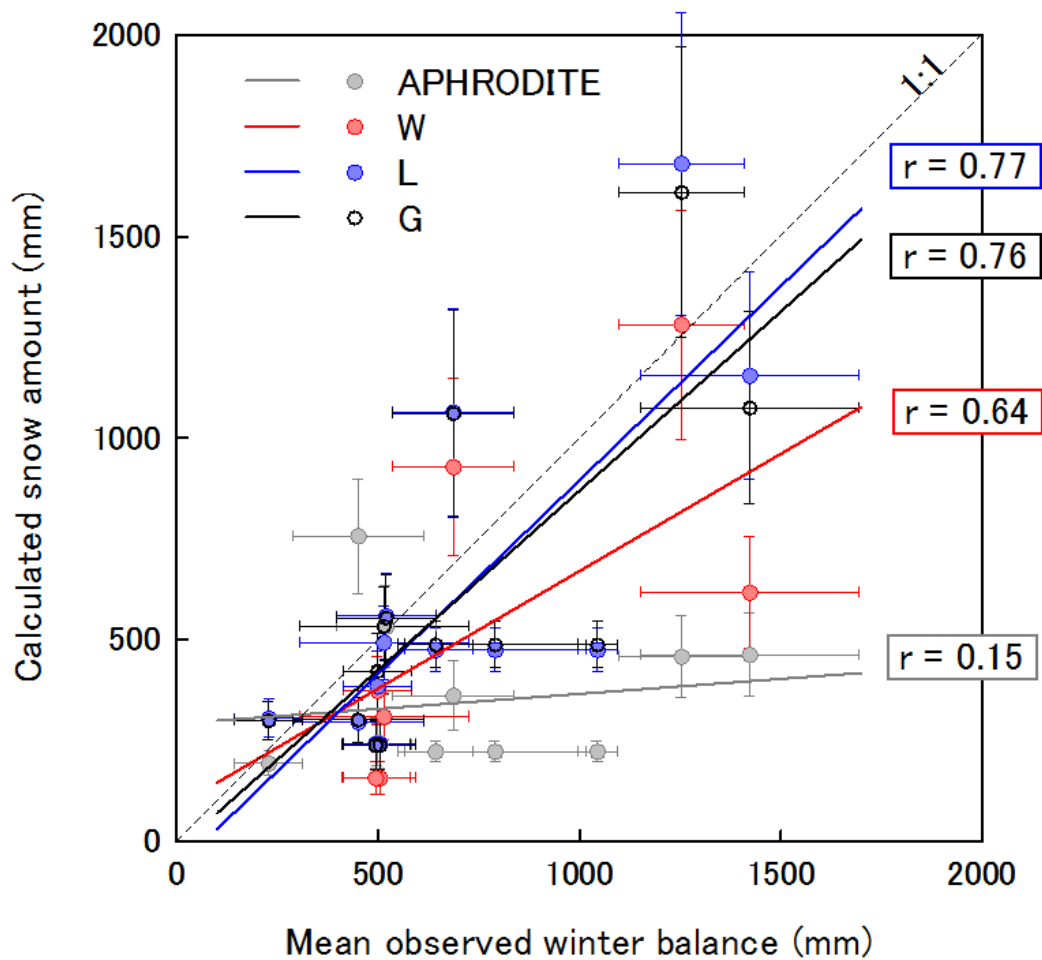


1

2 Fig. 6. Annual solid and liquid precipitation of APHRODITE averaged from 1979 to 2007 (a),
 3 at which a glacier was located in the GGI. Calculated annual precipitation assumed to
 4 accumulate on glacier surfaces based on (b) G-, (c) L-, and (d) W-average elevations.

5

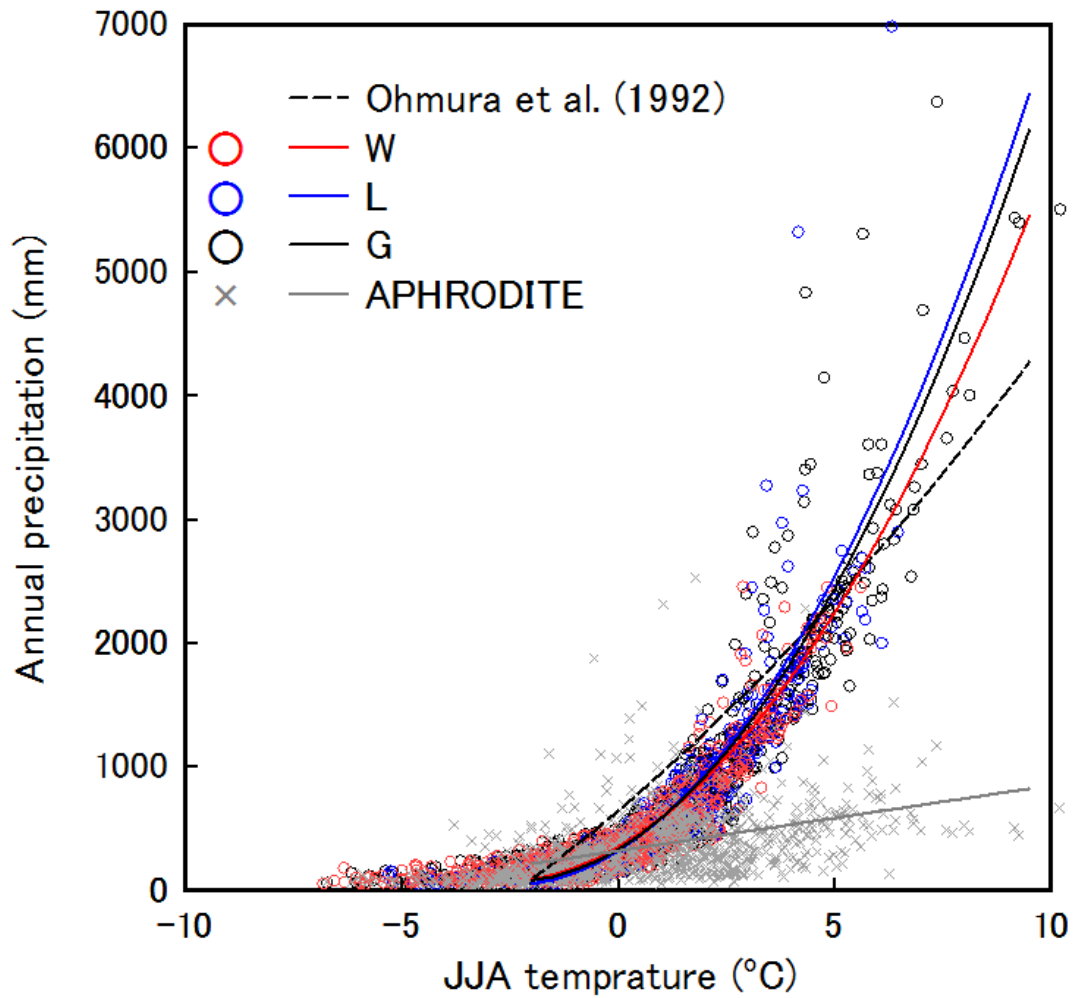
6



1
2

3 Fig. 7. Relation between observed winter balance averaged from 1979 to 2000 and calculated
 4 snow amounts. Grey circles indicate the snow amounts calculated from APHRODITE.
 5 Hollow small circles, blue circles, and red circles show those snow amounts calculated from
 6 precipitation based on G-average elevation, L-average elevation, and W-average elevation,
 7 respectively. Both vertical and horizontal error bars indicate standard deviation of each annual
 8 value. RMSE, correlation coefficient, and significance level between observed data and
 9 calculated snows are listed in Table S3.

10
11

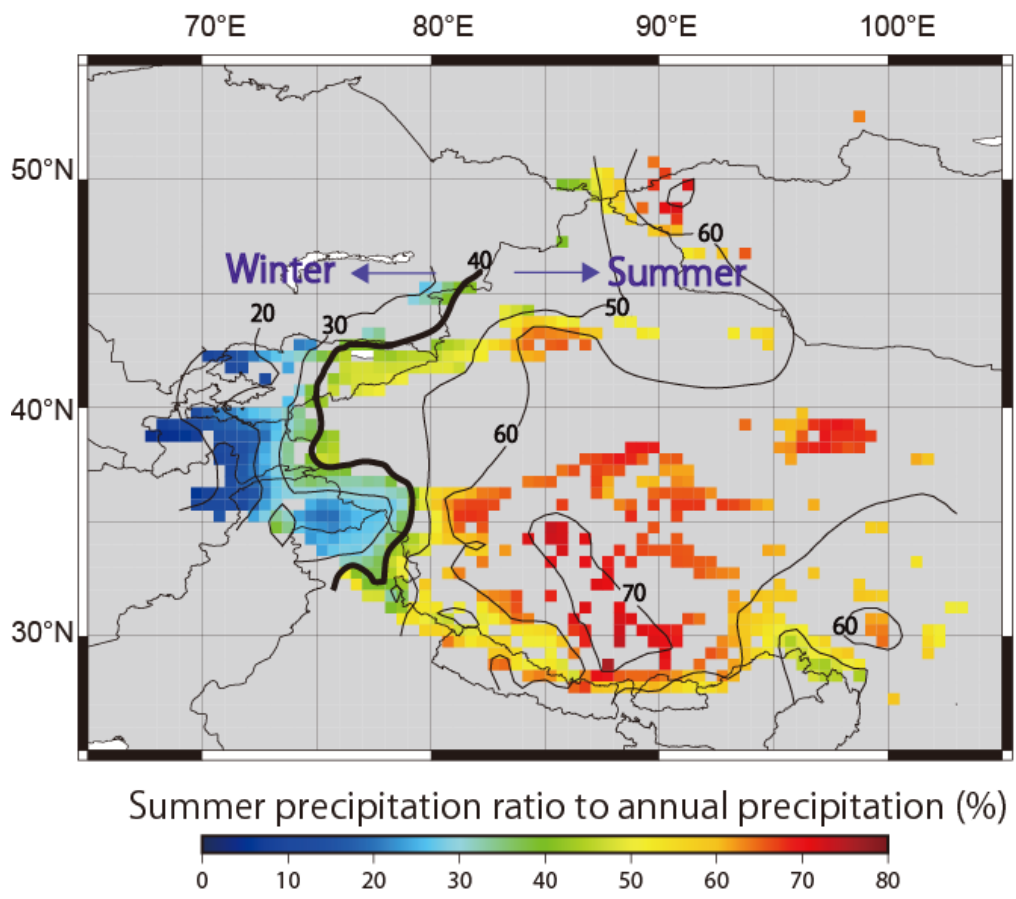


1

2 Fig. 8. Relation between summer (JJA) temperature and annual precipitation at G-median
 3 (black circles), L-average (blue circles), and W-average (red circles) elevations and
 4 APHRODITE averaged from 1979 to 2007 (grey crosses). Fitted curves of each dataset are
 5 plotted and shown by the respective colour. The fitted curve derived by Ohmura et al. (1992)
 6 is shown by the black dashed line.

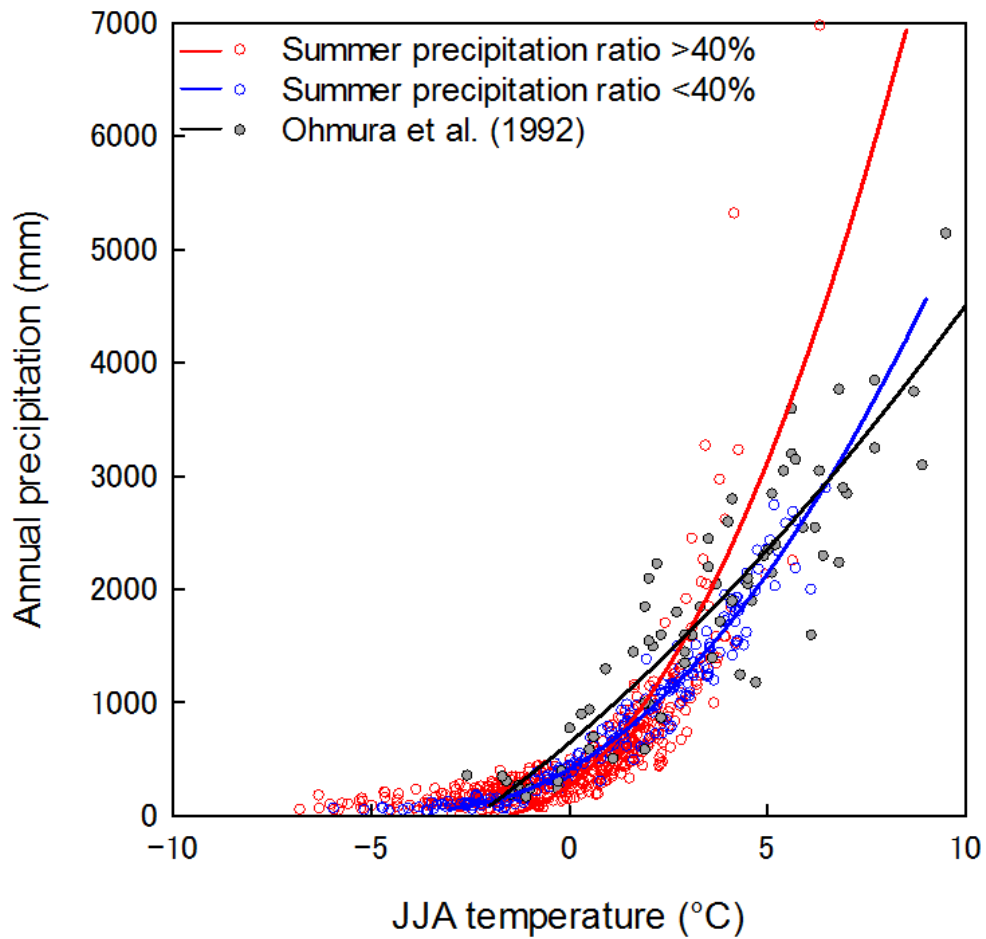
7

8



1
2
3
4
5
6
7

Fig. 9. Distribution of summer precipitation ratio to annual precipitation from APHRODITE data. Black thick line indicates the contour of the 40% summer precipitation ratio.



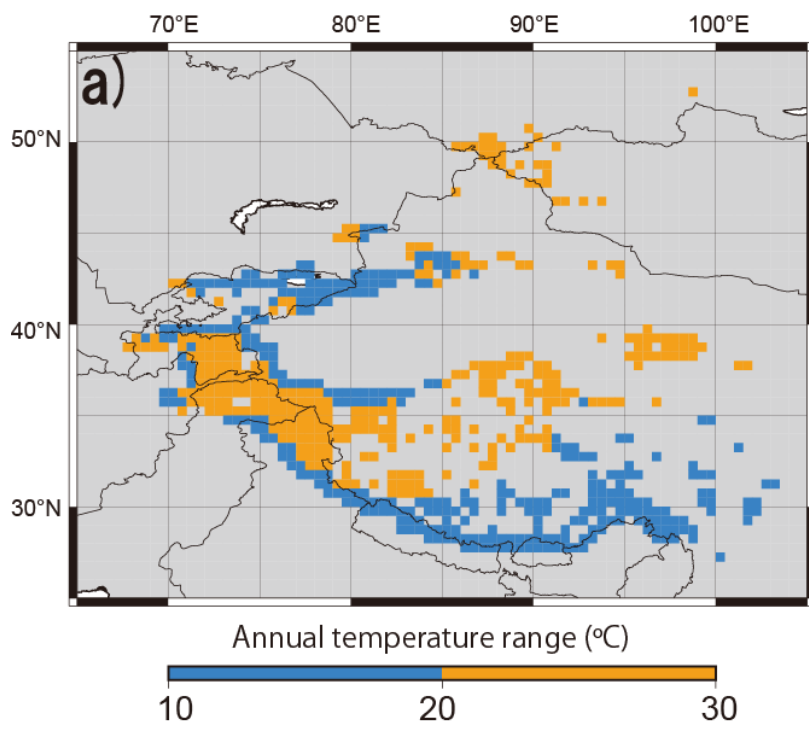
1

2

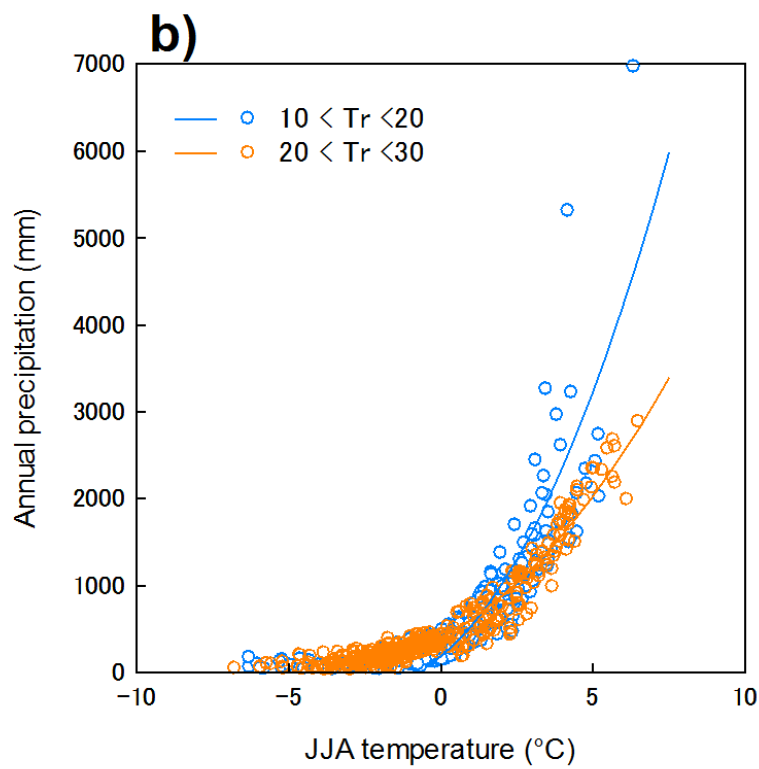
3 Fig. 10. Relation between mean summer (JJA) air temperature and annual precipitation at L-
 4 average elevation. Red and blue circles indicate summer-accumulation type and winter-
 5 accumulation type glaciers, respectively. Grey circles indicate the dataset reported by Ohmura
 6 et al. (1992).

7

8



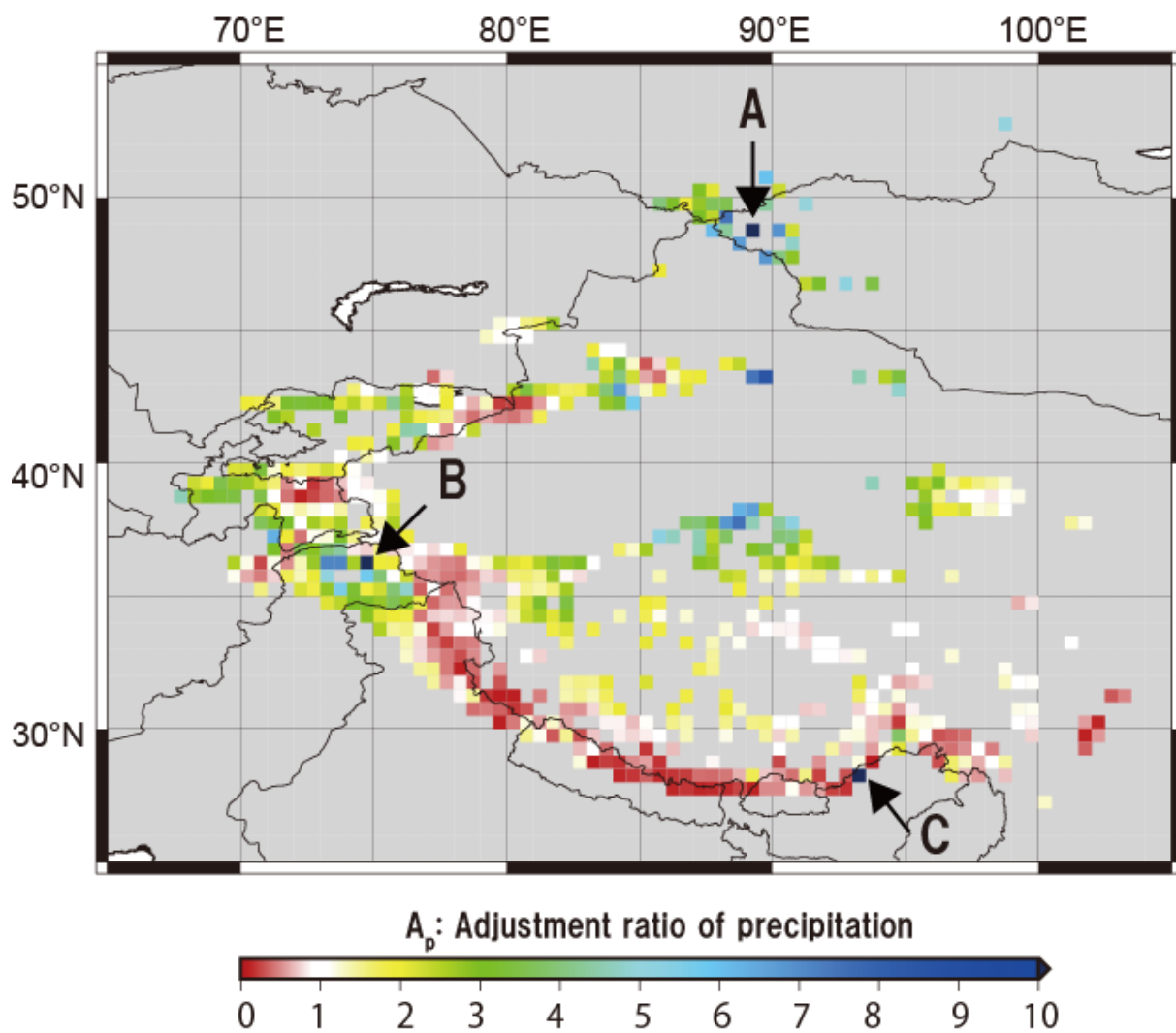
1



2

3 Fig. 11. Distribution of annual temperature range (a) and T-P plot of different temperature
 4 ranges. *Tr* indicates annual temperature range (b).

5



1
 2 Fig. 12. Distribution of the adjustment ratio of P_w to APHRODITE precipitation at each 0.5
 3 degree grid. Grids with adjustment ratio between 0.9 and 1.1 are indicated by white. A,B, and
 4 C indicate grid cells with large A_p (>10).
 5